

Relativistic excitation of compact stars

Zhiqiang Miao¹, Xuefeng Feng^{2,3}, Zhen Pan^{1,4} and Huan Yang^{5,*}

¹*Tsung-Dao Lee Institute, Shanghai Jiao Tong University, Shanghai, 1 Lisuo Road, 201210, China*

²*Fudan Center for Mathematics and Interdisciplinary Study, Fudan University, Shanghai, 200433, China*

³*Shanghai Institute for Mathematics and Interdisciplinary Sciences (SIMIS), Shanghai, 200433, China*

⁴*School of Physics & Astronomy, Shanghai Jiao-Tong University, Shanghai, 800 Dongchuan Road, 200240, China*

⁵*Department of Astronomy, Tsinghua University, Beijing 100084, China*

(Dated: July 1, 2025)

In this work, we study the excitation of a compact star under the influence of external gravitational driving in the relativistic regime. Using a model setup in which a wave with constant frequency is injected from past null infinity and scattered by the star to future null infinity, we show that the scattering coefficient encodes rich information of the star. For example, the analytical structure of the scattering coefficient implies that the decay rate of a mode generally plays the role of “star excitation factor”, similar to the “black hole excitation factor” previously defined for describing black hole mode excitations. With this star excitation factor we derive the transient mode excitation as a binary system crosses a generic mode resonance of a companion star during the inspiral stage. This application is useful because previous description of resonant mode excitation of stars still relies on the mode and driving force decomposition based on the Newtonian formalism. In addition, we show that the scattering phase is intimately related to the total energy of spacetime and matter under the driving of a steady input wave from infinity. We also derive the relevant tidal energy of a star under steady driving and compare that with the dynamic tide formula. We estimate that the difference may lead to $\mathcal{O}(0.5)$ radian phase modulation in the late stage of the binary neutron star inspiral waveform.

I. INTRODUCTION

Compact neutron star binaries are important sources for ground-based gravitational wave detection. Compared to black hole binaries, neutron stars contribute additional matter effects to the gravitational waveform, including (dynamic) tides [1, 2], mode resonances [3–14], and various post-merger signatures [15–22]. The post-merger stage usually takes place in the kilohertz range, so the associated gravitational wave emission is normally only observable with third-generation gravitational wave detectors [23–25]. In contrast, both dynamic tides and mode resonances occur during the inspiral stage with lower frequency. Their detection may inform us about the equation-of-state and the internal structure of neutron stars [1, 26–28].

Both effects are excited because of the gravitational force from the companion star. The current treatment of neutron star excitations assumes an effective model with one or more harmonic oscillators, and the external gravitational field is directly coupled to the oscillators [1–3]. Such a physical picture is justified in the Newtonian regime, as the fluid equation of motion within a star can be formally decomposed into a mode basis [3]:

$$\ddot{\xi}_n + \omega_n^2 \xi_n = \langle f, \psi_n \rangle \quad (1)$$

with ω_n being the eigenfrequency of the mode, ψ_n being the mode wavefunction, f being the external gravitational force, ξ_n being the time-dependent displacement of the

mode, $\langle \rangle$ being an inner product such that different modes are orthogonal to each other, and $\langle f, \psi_n \rangle$ being the overlap integral.

However, for a compact star in the fully relativistic regime, the local mass element of the star is still driven by the local gravitational perturbation, whereas the gravitational perturbation is both influenced by the external gravitational field and the fluid. In other words, it is no longer a good approximation to assume local gravitational perturbations by taking the values as if the star were not present. The gravitational perturbations and fluid perturbations must evolve and be computed consistently. Because the gravitational sector and the fluid sector are coupled, it is not clear whether the mode excitation can still be computed using the projection of external force. In fact, since generic modes have non-zero decay rates, they no longer form a complete set [29] and their wavefunctions are not orthogonal to each other using the vanilla inner product in Eq. (1).

Therefore, it is necessary to construct a formalism that applies in the fully relativistic regime. Earlier studies [30] extended the equilibrium tide calculation to a time-dependent regime by computing new tidal coefficients, but a complete theory describing the tidal dynamics of compact stars is still needed. In this work, we consider the excitation of a star with constant-frequency gravitational waves injected from past null infinity and scattered back to future null infinity. This setup describes generic time-dependent tidal drivings in the linear (amplitude) regime, as any time-dependent tidal driving can be Fourier decomposed into various frequency components. In addition, it can be shown that (see Sec. II) this wave-scattering problem is dual to the problem with a point

* hyangdoa@tsinghua.edu.cn

mass orbiting around the star, which can be considered as the extremal-mass-ratio limit of a binary problem. It is different but related to the treatment in [30] using dynamical Love numbers, which may be defined using the frequency expansion of our results.

With this scattering formalism we compute the scattering coefficient defined using the (complex) amplitudes of outgoing and ingoing waves at infinity, which encodes information about the tidal response of the star. The poles of the scattering coefficient correspond to quasinormal modes of the compact star. We argue that the poles and zeros of the scattering coefficient form conjugate pairs $\omega_R \pm i\omega_I$ in the complex frequency plane, which implies that the residue of a pole is well approximated by the imaginary part ω_I of the pole, if $\omega_I \ll \omega_R$. This observation provides remarkable simplification in understanding the black hole excitation factor, as detailed in Sec. II.

For a time-dependent driving field, the time-domain response of the star can be obtained by Fourier transforming its frequency-domain signal. We show that this naturally leads to transient excitations of quasinormal modes of the star, with information purely from the scattering coefficient, so that a mode projection procedure is no longer required. We further derive the transient energy of the modes in this relativistic regime, which agrees with its counterpart [3] in the Newtonian limit. The transient mode energy is generally proportional to the residue or the decay rate ω_I of the mode, which plays the role of an overlap integral between the mode wave function and the external gravitational field in Newtonian theory [Eq. (1)]. The residue is also analogous to the black hole excitation factor that describes the degree of black hole mode excitations in black hole ringdowns [31].

For a star under a steady external driving field, we show that the energy of gravitational and matter perturbations can be entirely determined by the amplitude of ingoing gravitational waves and the scattering angle of the outgoing wave. This is also numerically shown using the Hamiltonian of star perturbations derived in Refs. [32, 33]. However, the tidal energy of the star that enters the binary equation of motion is only part of the total energy. We employ the calculation first discussed in [34] to obtain the tidal energy of a compact star with a point mass orbiting in a circular orbit, and compare that with the prediction that was previously used assuming an effective tidal action in the Effective Field Theory approach and an effective mode description for the tidal action [2]. The relative difference ranges from zero to 3% if the inspiraling frequencies of a normal binary neutron star is $\leq 10^3$ Hz. Inaccuracy in the tidal energy may lead to a ~ 0.5 rad phase error in the gravitational waveform.

Therefore, the scattering formalism proves to be a powerful tool to describe the tidal response of stars under external gravitational drivings. With this formalism, both the transient mode energy and the dynamic tide energy can be computed accurately at the linear order of the external tidal gravitational field. This directly helps to improve the waveform accuracy in modeling matter effects

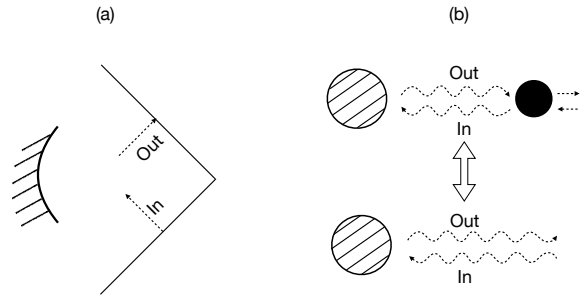


Figure 1. Schematic illustration of (a) Wave-scattering picture: gravitational waves are injected from past null infinity and scattered back to future null infinity by the star. (b) Duality between the wave-scattering picture and point-mass scenario.

in neutron star binaries. Combining with Post-Newtonian (PN) theory of nonlinear tides, a hybrid method may further reduce the model error. This will be particularly important for future observations with third-generation gravitational wave detectors, as the model systematics should be smaller than the detector noise to avoid biased measurements.

This paper is organized as follows. In Sec. II we introduce the wave-scattering formalism and discuss the duality between wave scattering and point-mass scenario, along with the definition of the external tidal field. In Sec. III, we provide a description of transient mode excitation in the relativistic regime. We derive the mode energy during resonant excitation and compare the results with the Newtonian case. Sec. IV focuses on the steady excitation of the f-mode. In Sec. IV A, we establish a flux balance law that connects the total perturbative energy in spacetime to the scattering phase. We then calculate the tidal energy using the self-force approach in the point-mass scenario in Sec. IV B, and incorporated it into the Effective-One-Body (EOB) framework in Sec. IV C. The results of tidal energy and the gravitational-wave phase shifts are discussed in Sec. IV D. We conclude in Sec. V.

II. SCATTERING FORMALISM

We consider a star with mass M and radius R . For simplicity, the star is assumed to be nonrotating, in which case the spacetime outside the star is Schwarzschild in the non-perturbed scenario. The gravitational perturbation in this vacuum exterior regime can be described by Regge-Wheeler-Zerilli formalism [35–37]. For a generic frequency component ω and in the limit that $r \rightarrow \infty$, the master variable Z has the asymptotic behavior:

$$Z(r \rightarrow \infty) = A_{\text{out}}(\omega)e^{i\omega r_*} + A_{\text{in}}(\omega)e^{-i\omega r_*} \quad (2)$$

where r_* is the tortoise coordinate. With the $e^{-i\omega t}$ factor restored it is just

$$Z(r \rightarrow \infty)e^{-i\omega t} = A_{\text{out}}(\omega)e^{i\omega u} + A_{\text{in}}(\omega)e^{i\omega v} \quad (3)$$

with $u := t - r_*$ and $v := t + r_*$.

Notice the ingoing piece of the wave A_{in} represents the external gravitational driving, and the response of the star is encoded in the complex scattering/reflection coefficient (see Fig. 1)

$$\mathcal{R} := \frac{A_{\text{out}}}{A_{\text{in}}}. \quad (4)$$

There are a few interesting properties of \mathcal{R} . First, for any real frequency ω , due to energy conservation, the ingoing energy flux has to be equal to the outgoing energy flux at infinity, which means that $|\mathcal{R}| = 1$. Second, the analytical structure of \mathcal{R} should look like

$$\mathcal{R} = \prod_n \frac{\omega - \omega_n^*}{\omega - \omega_n} \times [\text{nonpole component}] \quad (5)$$

with $\omega_n = \omega_{nR} - i\gamma_n$, $\omega_{-n} = -\omega_{nR} - i\gamma_n$ being the quasinormal mode frequencies. The zeros in the numerator are paired with poles of \mathcal{R} because under the time-reversal operation, we expect the role to switch between ingoing and outgoing waves, so that $\mathcal{R} \leftrightarrow 1/\mathcal{R}$.

The expression of Eq. (5) actually has non-trivial implications. Let us define the residue of \mathcal{R} at the pole with frequency ω_n as

$$\text{Res}[\mathcal{R}(\omega)] := W_n = \lim_{\omega \rightarrow \omega_n} (\omega - \omega_n)\mathcal{R}(\omega). \quad (6)$$

Notice that another way to write down the residue is

$$W_n = \frac{A_{\text{out}}}{dA_{\text{in}}/d\omega} \Big|_{\omega_n} = 2\omega_n \mathcal{B}_n, \quad (7)$$

where \mathcal{B}_n is the *black hole excitation factor* in black hole perturbation theory [31]. It should be generalized to star modes in the scenario considered here.

On the other hand, in the case that $\omega \approx \omega_n$, We may expand \mathcal{R} as

$$\begin{aligned} \mathcal{R} &= \frac{\omega - \omega_n^*}{\omega - \omega_n} \mathcal{R}_{0,n}(\omega) \\ &= \left(1 + \frac{2i\gamma_n}{\omega - \omega_n}\right) \mathcal{R}_{0,n}(\omega). \end{aligned} \quad (8)$$

Notice that $\mathcal{R}_{0,n}(\omega)$ no longer has a pole at ω_n , so that

$$W_n = 2i\gamma_n \mathcal{R}_{0,n}(\omega_n), \quad (9)$$

and

$$|W_n| = 2\gamma_n |\mathcal{R}_{0,n}(\omega_n)| \approx 2\gamma_n, \quad (10)$$

or

$$|\mathcal{B}_n| \approx \left| \frac{\gamma_n}{\omega_n} \right| \approx \frac{1}{Q_n}, \quad (11)$$

where Q_n stands for the mode quality factor. The last two equations hold for modes with $\gamma_n \ll \omega_{nR}$ and $\gamma_n \ll |\omega_n - \omega_m|$ for other modes with $m \neq n$. This ensures that $\mathcal{R}_{0,n}(\omega_n) \approx \mathcal{R}_{0,n}(\omega_{nR})$ is true as $|\mathcal{R}_{0,n}(\omega)| = 1$ is expected for real frequencies. Notice that the $\gamma_n \ll \omega_{nR}$ condition generally means that the amplitude of non-pole part of $\mathcal{R}_{0,n}$ is approximately one. If the condition $\gamma_n \ll |\omega_n - \omega_m|$ is not satisfied for certain mode m , we will need to take into the account the factor $|(\omega_n - \omega_m^*)/(\omega_n - \omega_m)|$ in the last equation of Eq. (10). Nevertheless, when the conditions are satisfied, we observe that *the (half) amplitude of the residue of mode n is essentially the decay rate of this mode, or the star excitation factor is the inverse of the mode quality factor.* The physical meaning of residue W_n will become clear in the discussion of transient mode energy in Sec. III, and the property shown in Eq. (10) will be useful to match the results with Newtonian scenarios.

In order to verify this point, we construct a series of $n = 1$ polytropic stars with the mass fixed to be $M = 1.4M_{\odot}$. Gravitational waves are injected from past null infinity and scattered by the star towards future null infinity. The details are presented in Appendices A and B. The decay rate of a particular mode is obtained by identifying the poles on the complex frequency plane. On the other hand, W_n is measured by numerically evaluating the residue around the pole. For the $\ell = 2$ f-mode, the comparison between $|W_n|/2$ and γ_n is presented in Fig. 2 for the selected series of star configurations. It is evident that the relative difference is on the 10^{-4} level.

As a side note, it turns out that this series-of-poles representation of the black hole excitation factor may also prove useful in understanding the spectral signatures of black holes. Consider a scenario where there are two poles ω_n, ω_m near each other for certain range of black hole parameters. In this case, Eq. (9) can be rewritten as

$$W_n = 2i\gamma_n \frac{\omega_n - \omega_m^*}{\omega_n - \omega_m} \mathcal{R}_{0,n,m}(\omega_n), \quad (12)$$

where $\mathcal{R}_{0,n,m}$ is a smooth function near ω_n . Since $|\omega_n - \omega_m| \ll |\omega_n|$, we find a large amplification factor in W_n and consequently the black hole excitation factor \mathcal{B}_n . This phenomenon has been observed numerically in the literature and is often referred to as the “mode avoidance and resonant excitation effect” [38–41]. The argument here provides a natural explanation for this phenomenon. It is also straightforward to see that $\mathcal{B}_n \approx -\mathcal{B}_m$ for sufficiently close poles, so the excitation of these two modes cancel largely with each other.

The scattering formalism exhibits the convenient property of encoding the tidal response of the star into the input/output relation at infinity. It is also connected to the scenario with a point mass orbiting around the same star, as depicted in Fig. 1. Inside the particle’s orbital radius, the vacuum solution of the Zerilli function can still be written as

$$Z(r) = A_{\text{out}} Z_{\text{out}}(r) + A_{\text{in}} Z_{\text{in}}(r), \quad (13)$$

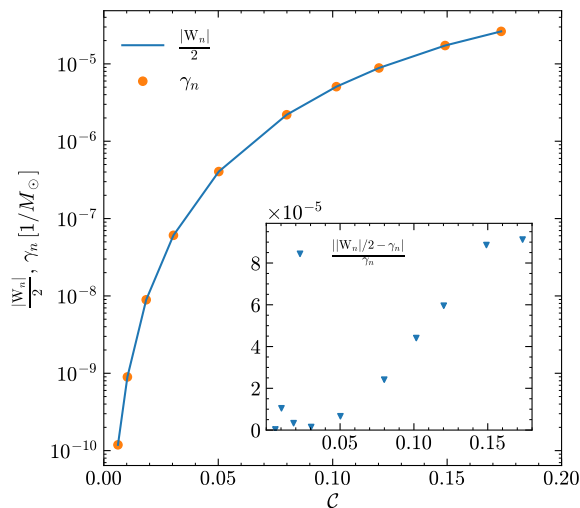


Figure 2. $|W_n|$ and γ_n as functions of stellar compactness, $\mathcal{C} := M/R$, for f-mode. The results are calculated from a set of stellar models using the polytropic equation of state with $n = 1$ and fixed stellar mass $M = 1.4 M_\odot$. The inset shows the relative difference between $|W_n|$ and γ_n .

where $Z_{\text{out},\text{in}}$ are the homogeneous solutions that satisfies the $e^{\pm i\omega r_*}$ asymptotic boundary condition at infinity. This implies that, within the wave-scattering picture, one can always fine-tune the amplitudes of the incoming and outgoing waves at infinity such that the solution inside the orbital radius matches the one obtained in the point-mass picture. Therefore, from the point of view of the star, whether it is driven by the gravitational field from a point mass or consistently tuned gravitational waves from infinity is indistinguishable from each other. There is always a wave-scattering problem that is dual to the point-mass scenario. We shall apply this view in studying the steady excitation of stars in Sec. IV.

A. Definition of the external tidal field

In the effective field theory description of tidally perturbed bodies, the internal degrees of freedom of each body couples with external tidal fields. Although the definition of external fields is not unique, it is reasonable to define it as the field as if the target body were removed from the spacetime. In the scenario where a point mass orbits around a star as considered here, the 'external field' of the star may be characterized by its 'equivalent' amplitude A_{in} at null infinity, according to the mapping relation shown in panel (b) of Fig. 1. If the star were to be removed from spacetime, one can evaluate the value of the tidal tensor \mathcal{E}_{ij} at $r = 0$ assuming the same incoming wave amplitude at infinity. This defines an operational procedure to obtain the external tidal field for the model problem considered here, which allows us to compare the results measured both in A_{in} and in \mathcal{E}_{ij} .

As mentioned above, the ingoing wave acts as the external gravitational driving. Therefore, we can define the external tidal field in terms of the ingoing wave amplitude A_{in} . Since this definition is independent of the nature of the central object, we consider the perturbations in Minkowski spacetime for simplicity. The perturbed metric in Regge-Wheeler gauge is given by [35–37]

$$ds^2 = -dt^2 + dr^2 + r^2(d\theta^2 + \sin^2\theta d\phi^2) + \left[H_0(dt^2 + dr^2) + 2i\omega r H_1 dt dr + Kr^2(d\theta^2 + \sin^2\theta d\phi^2) \right] Y_{\ell m}(\theta, \phi) e^{-i\omega t}, \quad (14)$$

and the Zerilli equation reduces to

$$\frac{d^2 Z}{dr^2} + \left[\omega^2 - \frac{\ell(\ell+1)}{r^2} \right] Z = 0, \quad (15)$$

where

$$K = \frac{n+1}{r} Z + \frac{dZ}{dr}, \quad (16)$$

$$H_1 = -\frac{Z}{r} - \frac{dZ}{dr}, \quad (17)$$

$$H_0 = -\frac{1}{n} [(\omega^2 r^2 - n)K + \omega^2 r^2 H_1], \quad (18)$$

$$n = \frac{(\ell-1)(\ell+2)}{2}. \quad (19)$$

The regular solution of Zerilli variable is $Z = A\omega r j_\ell(\omega r)$, which has the asymptotic behavior at spatial infinity,

$$Z(r \rightarrow \infty) = \frac{A}{2i} e^{i(\omega r - \ell\pi/2)} - \frac{A}{2i} e^{-i(\omega r - \ell\pi/2)}, \quad (20)$$

from which the ingoing wave amplitude reads

$$A_{\text{in}} = -\frac{A}{2i} e^{i\ell\pi/2}. \quad (21)$$

Substituting the solution of Z into Eq. (18) and taking the $r \rightarrow 0$ limit, we get

$$H_0(r \rightarrow 0) = A\omega \left[(n+2)j_\ell(\omega r) + r \frac{dj_\ell(\omega r)}{dr} \right] = \frac{(\ell+1)(\ell+2)}{2(2\ell+1)!!} A\omega^{\ell+1} r^\ell + \mathcal{O}(r^{\ell+1}). \quad (22)$$

The external tidal field can be decomposed as

$$\mathcal{E}_L = \sum_{m=-\ell}^{\ell} \mathcal{E}_{\ell m} \mathcal{Y}_L^{\ell m}, \quad (23)$$

where the symmetric traceless tensor $\mathcal{Y}_L^{\ell m}$ is defined by

$$Y_{\ell m}(\theta, \phi) = \mathcal{Y}_L^{\ell m} n^L, \quad (24)$$

with $\mathbf{n} = (\sin\theta \cos\phi, \sin\theta \sin\phi, \cos\theta)$. L denotes a string of indices on a symmetric trace-free tensor, for example

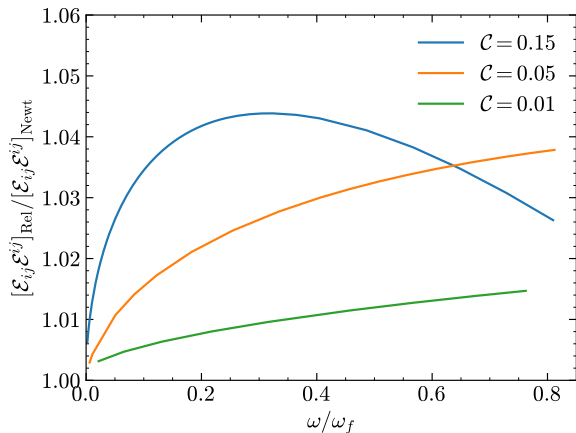


Figure 3. The ratio between the amplitude-based [Eq. (29)] and Newtonian definitions ($[\mathcal{E}_{ij}\mathcal{E}^{ij}]_{\text{Newt}} = \frac{9}{4}(\frac{m_2}{m_1+m_2})^2\Omega^4$) of external tidal field as function of the GW frequency $\omega = m\Omega$ for $(\ell, m) = (2, 2)$ mode. ω_f is the f-mode frequency.

$n^{L=2} = n^i n^j - \frac{1}{3}\delta^{ij}$. In our simplified case, the time-time metric component has the form [42]

$$\frac{1 + g_{tt}}{2} = \sum_{\ell} -\frac{1}{\ell!} r^{\ell} \mathcal{E}_L n^L, \quad (25)$$

from which we can read the (ℓ, m) part of the tidal tensor through

$$-\frac{1}{\ell!} r^{\ell} \mathcal{E}_{\ell m} Y_{\ell m} = \frac{1}{2} H_0 Y_{\ell m}. \quad (26)$$

The result is

$$\mathcal{E}_{\ell m} = -\frac{(\ell+1)(\ell+2)\ell!}{4(2\ell+1)!!} A\omega^{\ell+1}, \quad (27)$$

and

$$\mathcal{E}_L \mathcal{E}^L|_{\ell m} = \frac{(\ell+1)(\ell+2)(\ell+2)!}{16\pi(2\ell+1)!!} |A_{\text{in}}|^2 \omega^{2\ell+2}. \quad (28)$$

For the $(\ell, m) = (2, 2)$ mode, we have

$$\mathcal{E}_{ij}\mathcal{E}^{ij}|_{\ell m=22} = \frac{6}{5\pi} |A_{\text{in}}|^2 \omega^6. \quad (29)$$

In Fig. 3, we compare the external tidal field defined via the ingoing amplitude extracted from perturbation calculations of the point-mass scenario (see Appendix C) with the Newtonian results. The difference between the amplitude-based definition and the Newtonian case is found to be at the 10^{-2} level.

III. TRANSIENT EXCITATION

In Newtonian theory, the excitation of modes of a star can be described via Eq. (1), which relies on the

projection of external gravitational force into a mode basis. However, in the relativistic regime the wavefunction of an eigenmode of a star is generally defined in the entire spacetime domain, as the modes radiate. In addition, modes do not form a complete basis for relativistic stars. As a result, it is not necessarily clear how to promote the inner product in Eq. (1) to the relativistic regime. Note that for black holes, a bilinear form can be defined to ensure mode orthogonality behavior [43]. It is still unknown whether or how a similar construction may be achieved for stars.

In this section, we adopt an alternative approach. We show that the transient mode excitation can already be described with the input/output relation in the wave-scattering scenario. We compute the transient mode energy as an evolving binary sweeps through the frequency of a resonant mode in Sec. III A, and show that it is indeed consistent with the known Newtonian formula in the Newtonian regime in Sec. III B. The difference between the Newtonian description and the relativistic description is discussed in Sec. III C.

A. Deriving the transient mode excitation

In order to model a time-dependent driving field, we promote the ingoing gravitational wave in the scattering formalism to be time-dependent. Let us consider the case that the driving frequency slowly shifts in time, $\dot{\sigma} \ll \sigma^2$ (In this subsection, we denote the driving frequency by σ to avoid confusion with the Fourier frequency ω):

$$A_{\text{in}}(t) = A_{\text{in},0} e^{-i \int^t dt' \sigma(t')}, \quad (30)$$

so that

$$\begin{aligned} A_{\text{in}}(\omega) &= A_{\text{in},0} \int dt_1 e^{i\omega t_1} e^{-i \int_0^{t_1} dt' \sigma(t')} \\ &= A_{\text{in},0} \int dt_1 e^{i \int_0^{t_1} dt' (\omega - \sigma(t'))}. \end{aligned} \quad (31)$$

We define a characteristic time t_{ω} that is associated to the driving frequency σ via $\sigma(t_{\omega}) = \omega$. For t close to t_{ω} , $\sigma(t)$ can be expanded as $\sigma(t) = \omega + \dot{\sigma} \Delta t$ ($\Delta t := t - t_{\omega}$). Plugging in these simplification into Eq. (31) we get

$$\begin{aligned} A_{\text{in}}(\omega) &= A_{\text{in},0} e^{i\Phi_{\omega}} \int d\Delta t e^{i\dot{\omega} \Delta t^2/2} \\ &= A_{\text{in},0} e^{i\Phi_{\omega}} (1+i) \sqrt{\frac{\pi}{\dot{\sigma}}}, \end{aligned} \quad (32)$$

where $\Phi_{\omega} = \int_0^{t_{\omega}} dt' (\omega - \sigma(t'))$. In the frequency domain we still have the input-output relation with

$$A_{\text{out}}(\omega) = \mathcal{R}(\omega) A_{\text{in}}(\omega), \quad (33)$$

where $\mathcal{R}(\omega)$ is essentially the Fourier transform of the transfer function. The outgoing wave in the time domain

is given by

$$A_{\text{out}} = \frac{1}{2\pi} \int_{-\infty}^{\infty} d\omega e^{-i\omega t} \mathcal{R}(\omega) A_{\text{in}}(\omega). \quad (34)$$

For sufficiently late t we close the contour on the lower half-plane, and the poles of $\mathcal{R}(\omega)$ give rise to the quasi-normal mode part of A_{out} , where the direct part and tail part are not the focus here. We have

$$\begin{aligned} A_{\text{out,mode}} &= \frac{1+i}{2\pi} \sqrt{\frac{\pi}{\dot{\sigma}}} A_{\text{in},0} \sum_n e^{-i \int^{t\omega_n} dt' \sigma(t')} 2\pi i W_n e^{-i\omega_n(t-t\omega_n)} \\ &\approx \frac{1+i}{2\pi} \sqrt{\frac{\pi}{\dot{\sigma}}} A_{\text{in},0} \sum_n e^{-i \int^{t\omega_{nR}} dt' \sigma(t')} 2\pi i W_n e^{-i\omega_n(t-t\omega_n)} \\ &= \frac{1+i}{2\pi} \sqrt{\frac{\pi}{\dot{\sigma}}} \sum_n A_{\text{in}}(t\omega_{nR}) 2\pi i W_n e^{-i\omega_n(t-t\omega_n)}, \end{aligned} \quad (35)$$

for modes sufficiently close to the real axis. In this way we can find out the amplitude of freely excited modes after transient resonances.

This can already be used to obtain the transient energy of a single mode. After a certain mode is resonantly excited, the presence of a mode piece $A_{\text{out,mode},n}$ contributes additional flux in the outgoing radiation. This free-mode piece (with frequency $\omega_{nR} - i\gamma_n$) should quickly dephase with the evolving orbital frequency σ . Physically this corresponds to a free mode of star excited in addition to the driven oscillation. Notice that the energy of a free mode can be computed from its corresponding integrated flux at infinity:

$$\begin{aligned} E_{\text{mode, Rel}} &= C_{\omega_{nR}} \int_{t\omega_n}^{\infty} dt |A_{\text{out,mode},n}|^2 \\ &= C_{\omega_{nR}} \frac{2\pi |W_n|}{\dot{\sigma}} |A_{\text{in}}(t\omega_{nR})|^2 \\ &= \frac{1}{32} \frac{(\ell+2)!}{(\ell-2)!} \frac{|W_n|}{\dot{\sigma}} |A_{\text{in}}(t\omega_{nR})|^2 \omega_{nR}^2, \end{aligned} \quad (36)$$

where we have used Eq. (10) and the geometric factor C_ω is given by [37]

$$C_\omega = \frac{1}{64\pi} \frac{(\ell+2)!}{(\ell-2)!} \omega^2. \quad (37)$$

In fact, the problem can also be understood from an alternative perspective. The resonance occurs over a finite time interval of duration $\Delta t \sim \sqrt{1/\dot{\sigma}}$, centered around the resonance point ($\sigma(t\omega_{nR}) = \omega_{nR}$). During this period, energy transfer takes place due to the beating between the driven and free components, which is imprinted as an interference pattern in the outgoing radiation. The energy deposited into the mode during resonance can be

directly computed from

$$\begin{aligned} E_{\text{mode, Rel}} &= \int_{t_1}^{t_2} C_\sigma (|A_{\text{in}}(\sigma)|^2 - |A_{\text{out}}(\sigma)|^2) dt \\ &= \int_{\sigma_1}^{\sigma_2} C_\sigma |A_{\text{in}}(\sigma)|^2 [1 - |R(\sigma)|^2] \frac{1}{\dot{\sigma}} d\sigma \\ &= \int_{\sigma_1}^{\sigma_2} C_\sigma |A_{\text{in}}(\sigma)|^2 \frac{4\gamma_n^2}{(\sigma - \omega_{nR})^2 + \gamma_n^2} \frac{1}{\dot{\sigma}} d\sigma \\ &\approx C_{\omega_{nR}} |A_{\text{in}}(\omega_{nR})|^2 \frac{1}{\dot{\sigma}} \int_{-\infty}^{\infty} \frac{4\gamma_n^2}{(\sigma - \omega_{nR})^2 + \gamma_n^2} d\sigma \\ &= C_{\omega_{nR}} |A_{\text{in}}(\omega_{nR})|^2 \frac{4\pi\gamma_n}{\dot{\sigma}} \\ &= \frac{1}{16} \frac{(\ell+2)!}{(\ell-2)!} \frac{\gamma_n}{\dot{\sigma}} |A_{\text{in}}(\omega_{nR})|^2 \omega_{nR}^2. \end{aligned} \quad (38)$$

In the third line, we have used the analytic structure of \mathcal{R} near the mode pole, as given in Eq. (8), which implies that $1 - |\mathcal{R}(\sigma)|^2$ takes a Lorentzian form centered at $\sigma = \omega_{nR}$ with width γ_n . In the fourth line, we extended the integration limits to $(-\infty, \infty)$, justified by the fact that the contribution of the integral comes from frequency interval $\sim \gamma_n$, which is much less than the resonance width, i.e., $\sigma_2 - \sigma_1 \sim \sqrt{\dot{\sigma}} \gg \gamma_n$. Meanwhile, the integral can be approximated by its value at the resonance point, i.e., $C_\sigma \approx C_{\omega_{nR}}$ and $|A_{\text{in}}(\sigma)|^2 \approx |A_{\text{in}}(\omega_{nR})|^2$. It is obvious Eq. (38) agree with Eq. (36). This calculation also confirms the understanding that external driving deposits the resonant mode energy $E_{\text{mode, Rel}}$ to the star during the transient resonance period, which is later on carried away by gravitational wave radiation.

The transient energy of the modes is directly proportional to $|W_n|$, which is proportional to the damping rate of the mode γ_n . For a normal neutron star with mass $\sim 1.4 M_\odot$ and radius ~ 13 km, the ratio between γ_n and ω_{nR} is $\sim 10^{-3}$ for a $\ell = 2$ f-mode and 10^{-14} for a $\ell = 2$ g₁-mode. Therefore, it is computationally challenging to calculate $|W_n|$ for various modes. In Appendix B and Appendix F, we illustrate two independent approaches for computing $|W_n|$: the method discussed in Appendix B is based on a direct evaluation of the residue around the pole, and the method discussed in Appendix F is motivated by the eigenvalue perturbation theory [43, 44].

As Eq. (36) generally applies for various kinds of mode excitation during a binary inspiral process, it is instructive to compute $|W_n|$ of various relevant modes discussed in the literature. This systematic mode characterization will be studied in a separate work.

B. Newtonian limit

In the Newtonian regime, we may reexpress Eq. (1) as

$$\ddot{a}_n + \omega_n^2 a_n = -\frac{\mathcal{E}_{\ell m} Q_{n\ell m}}{\ell!}, \quad (39)$$

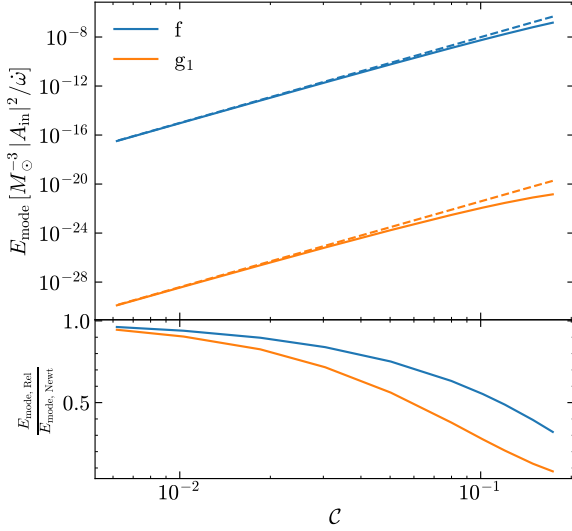


Figure 4. Top: Transient mode energy of f-mode (blue) and g_1 -mode (orange) resonance as a function of the stellar compactness \mathcal{C} . Both results calculated from the relativistic formula [Eq. (36), solid] and the Newtonian formula [Eq. (42), dashed] are plotted. The stellar models are constructed from polytropic equation of state with $n = 1$. Bottom: Comparison of the transient energy between the two formula.

where a_n is the mode amplitude. The tidal overlap integral is defined as usual [3],

$$Q_{n\ell m} = \int \ell r^{\ell+1} [\xi_n^r + (\ell+1)\xi_n^\perp] dr, \quad (40)$$

with $\xi_n = (\xi_n^r e_r + \xi_n^\perp r \nabla_\perp) Y_{\ell m}$ is the mode wavefunction. After the resonance, we expect a_n to oscillate at its own eigenfrequency ω_n , thus it is more appropriate to define a function c_n such that $a_n = c_n e^{-i\omega_n t}$. Plugging c_n into Eq. (39) and dropping the \ddot{c}_n term, we get

$$c_n = \frac{1}{2i\omega_n} \frac{\mathcal{E}_{\ell m} Q_{n\ell m}}{\ell!} \int e^{i\omega t^2/2} dt = \frac{1+i}{2i\omega_n} \frac{\mathcal{E}_{\ell m} Q_{n\ell m}}{\ell!} \left(\frac{\pi}{\dot{\omega}}\right)^{1/2}, \quad (41)$$

where we have used the stationary phase approximation. The resonant mode energy is then obtained with

$$\begin{aligned} E_{\text{mode, Newt}} &= \omega_n^2 |a_n|^2 \\ &= \frac{\pi}{2\dot{\omega}} Q_{n\ell m}^2 \frac{\mathcal{E}_{\ell m}^2}{(\ell!)^2} \\ &= \frac{\pi}{2\dot{\omega}} Q_{n\ell m}^2 \left[\frac{(\ell+2)(\ell+1)}{2(2\ell+1)!!} \right]^2 |A_{\text{in}}|^2 \omega_n^{2\ell+2}. \end{aligned} \quad (42)$$

On the other hand, if we consider a damped mode with the amplitude $a_n = c_n e^{-i\omega_n t - \gamma_n t}$, the mode energy is

$$E_{\text{mode, Newt}} = \omega_n^2 |c_n|^2 e^{-2\gamma_n t}. \quad (43)$$

The mode damping due to GW radiation can also be

approximated using the multipole formula [42],

$$\begin{aligned} \frac{dE_{\text{mode, Newt}}}{dt} &= - \frac{(\ell+1)(\ell+2)}{\ell(\ell-1)\ell!(2\ell+1)!!} \langle I_L^{(\ell+1)} I_L^{(\ell+1)} \rangle \\ &= - \frac{4\pi(\ell+1)(\ell+2)}{\ell(\ell-1)[(2\ell+1)!!]^2} Q_{n\ell m}^2 \omega_n^{2\ell+2} |a_n|^2 \\ &= - \frac{4\pi(\ell+1)(\ell+2)}{\ell(\ell-1)[(2\ell+1)!!]^2} Q_{n\ell m}^2 \omega_n^{2\ell+2} |c_n|^2 e^{-2\gamma_n t}, \end{aligned} \quad (44)$$

Combining Eq. (44) with Eq. (43), we deduce the decay rate to be

$$\gamma_n = \frac{2\pi}{[(2\ell+1)!!]^2} \frac{(\ell+1)(\ell+2)}{\ell(\ell-1)} Q_{n\ell m}^2 \omega_n^{2\ell}. \quad (45)$$

Plugging Eq. (45) into Eq. (42), we find

$$E_{\text{mode, Newt}} = \frac{1}{16} \frac{(\ell+2)!}{(\ell-2)!} \frac{\gamma_n}{\dot{\omega}} |A_{\text{in}}|^2 \omega_n^2. \quad (46)$$

In Sec. III A, we have computed the energy gained by stellar modes during resonant excitation in the fully relativistic regime, $E_{\text{mode, Rel}}$, as given by Eq. (36) [or Eq. (38)]. We expect that in the Newtonian limit these expressions should reduce to the energy derived in the Newtonian framework presented in this subsection $E_{\text{mode, Newt}}$. A direct comparison between Eq. (36) (or Eq. (38)) and Eq. (46) clearly shows that the Newtonian limit is correctly recovered (see also Fig. 4). In the next subsection, we will numerically compare $E_{\text{mode, Rel}}$ and $E_{\text{mode, Newt}}$ for stars with different compactness, highlighting the deviations between the two formulas.

C. Comparison with Newtonian stars for f-mode and g-mode resonances

In this subsection, we present illustrative comparisons of the transient mode energy associated with f-mode and g-mode resonances between relativistic and Newtonian stars. Notice that the f-mode is unlikely to be fully excited in a realistic binary.

We adopt a set of energy-polytrope equations of state to construct the stellar model, i.e.,

$$p = \kappa \varepsilon^{1+1/n}, \quad (47)$$

where p is the pressure and ε is the energy density. We set $n = 1$ in this work for simplicity. We then fix the stellar mass to $M = 1.4 M_\odot$, and vary the parameter κ to adjust the stellar radius R , thus producing stars with different compactness $\mathcal{C} := M/R$. In this way, we construct a set of relativistic stars and a corresponding set of Newtonian stars, each spanning a range of stellar compactness. To model the stratification relevant to g-modes, we also consider a parameterized setup with $\Gamma = \gamma(1 + \delta)$, where for relativistic stars

$$\gamma := \frac{p + \varepsilon}{p} \frac{dp}{d\varepsilon}, \quad (48)$$

$$\Gamma := \frac{p + \varepsilon}{p} \left(\frac{\partial p}{\partial \varepsilon} \right)_s. \quad (49)$$

Here, the subscript “s” indicates that the partial derivative is taken at constant composition (i.e., no change in entropy or chemical makeup). Physically, γ is the adiabatic index associated with the equilibrium structure, while Γ governs the response of the stellar fluid to pulsational compressions with no composition change. The difference $\Gamma - \gamma$ quantifies the degree of stable stratification in the stellar interior, which are essential for the existence and behavior of g-modes. We take $\delta = 0.005$ in our calculation.

The mode calculations for relativistic stars are provided in Appendices A & B, while the mode calculations for Newtonian stars can be found elsewhere (e.g., Ref. [3]). Here, we only compute the f-mode and g_1 -mode for $\ell = 2$. We then use Eq. (36) to calculate the transient mode energy for relativistic stars, while use Eq. (42) to calculate it for Newtonian stars. The results are plotted in Fig. 4. As the compactness approaches zero (the Newtonian limit), the energy computed from the relativistic formalism agrees well with the Newtonian result. However, as the stellar compactness increases, the transient energy predicted by the relativistic formalism becomes significantly lower than that of the Newtonian case. For typical neutron star compactness ($C \sim 0.15$), the energy associated with the resonances in the f-mode and g_1 -mode is reduced by approximately $\sim 60\%$ and $\sim 90\%$, respectively, compared to the Newtonian case. This means that a Newtonian calculation for the mode energy may receive a systematic error of up to one order of magnitude. As W_n is proportional to the square of the “overlap integral” between the external tidal field and mode wavefunction, it suggests that similar overlap functions, such as those used for computing nonlinear mode-coupling coefficients, may also receive significant relativistic correction. In order to accurately describe the resonant mode excitations, it is necessary to adopt the description in the relativistic regime.

IV. STEADY EXCITATION

In this section, we discuss how steady excitation of modes can be described using the input-output relation within the wave scattering framework. We begin by establishing a flux balance law which connects the total energy stored in the system to the scattering phase. We numerically verify this formula using the Hamiltonian of a compact star derived in [32, 33]. In the second part, we discuss an alternative way of computing the tidal energy of a binary containing compact star(s), motivated by gravitational self-force, and compare the predictions with those from an effective field description, which has been widely used in the previous literature.

A. Flux balance law

Considering a star driven by a steady strain of ingoing gravitational waves as depicted in Fig. 1, one important question is what the total energy (associated with the driving field) within the spacetime should be. Notice that for characterizing the tidal effects within the inspiral waveform, currently the tidal energy of a deformed neutron star within a binary is computed by an effective field theory approach (see, e.g. [2]), where all the degrees of freedom are summarized into one single mode. It is necessary to understand the systematic error associated with this effective one-mode approach by a direct comparison with a relativistic calculation.

According to the discussion in [32, 33], the energy associated with perturbations in a Schwarzschild spacetime and the energy associated with (fluid and gravitational) perturbations of a compact star can be derived in a Hamiltonian formalism. Alternatively, we shall show that the information about the energy of the star is also encoded in the phase of the scattered wave, which can be found from the input-output relation. Two descriptions actually lead to the same result, as demonstrated from numerical examples.

Let us start with the analysis within the input-output formalism. In order to compute the energy at the steady state, it is instructive to consider a “ramping-up” stage where the field increases from zero to the steady value, and the energy of the spacetime should be equal to the net flux injected from infinity. This can be achieved by assuming a small change in driving frequency, $\omega \rightarrow \omega + i\epsilon$, such that the time dependence of the waves becomes $e^{-i\omega t} e^{\epsilon t}$, corresponding to a slowly growing amplitude. In this case, the outgoing amplitude takes the form

$$A_{\text{out}} = A_{\text{in}} \mathcal{R}(\omega + i\epsilon) = A_{\text{in}} \left[\mathcal{R}(\omega) + \frac{\partial \mathcal{R}}{\partial \omega} i\epsilon \right]. \quad (50)$$

Imagine $A_{\text{in},0}$ is an initial ingoing amplitude and it takes a long time t to grow to the current amplitude $A_{\text{in},t}$:

$$A_{\text{in},t} = e^{\epsilon t} A_{\text{in},0}. \quad (51)$$

Then the total energy injected into the system should be equal to the accumulated differential flux over time, i.e.,

$$\begin{aligned} E_{\text{tot}} &= C_\omega \int^t dt (|A_{\text{in},t}|^2 - |A_{\text{out},t}|^2) \\ &= C_\omega \int^t dt |A_{\text{in},t}|^2 (1 - |\mathcal{R}(\omega + i\epsilon)|^2) \\ &= -i C_\omega \int^t \epsilon dt |A_{\text{in},0}|^2 e^{2\epsilon t} \left(\mathcal{R}^* \frac{\partial \mathcal{R}}{\partial \omega} - \mathcal{R} \frac{\partial \mathcal{R}^*}{\partial \omega} \right) \\ &= -i \frac{C_\omega}{2} \left(\mathcal{R}^* \frac{\partial \mathcal{R}}{\partial \omega} - \mathcal{R} \frac{\partial \mathcal{R}^*}{\partial \omega} \right) |A_{\text{in},t}|^2. \end{aligned}$$

Reexpressing $\mathcal{R}(\omega)$ as $|\mathcal{R}(\omega)| e^{i\theta}$ ($|\mathcal{R}(\omega)| = 1$ for real ω), we then obtain

$$E_{\text{tot}} = C_\omega \frac{\partial \theta}{\partial \omega} |A_{\text{in},t}|^2, \quad (52)$$

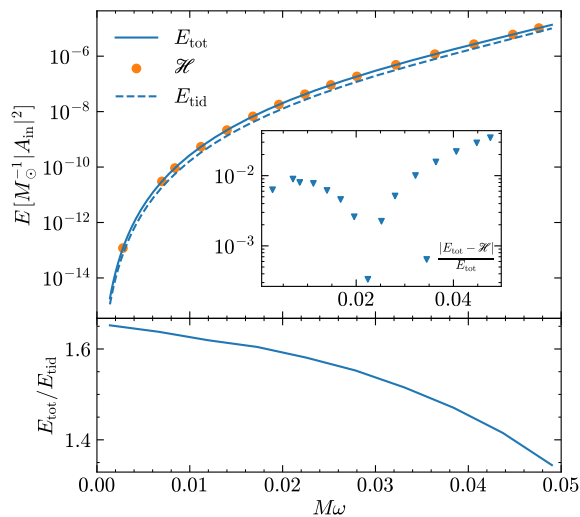


Figure 5. Comparison between the total energy obtained from the input-output formalism (E_{tot}) and the energy derived from the Hamiltonian formalism (\mathcal{H}). The Compact star/Black hole mass is fixed at $M = 1.4 M_{\odot}$. Also shown is the tidal energy E_{tid} . The inset shows the relative difference between E_{tot} and \mathcal{H} .

from which we see that the total energy is proportional to the derivative of the scattering phase. It should be noted that in Eq. (52), the definition of total energy includes an arbitrary zero-point freedom. Physically it corresponds to the “free-propagation” time or phase that is not associated with the tidal response of the central object. In the analysis in [45] for the tidal response of black holes, a far-zone phase θ_{far} is removed due to similar reasons. To remove this degree of freedom, we may consider the energy difference between two systems (I and II) that have the same external spacetime if there is no external perturbations, because the far-zone phase should be the same for these two systems. Since in this work we are interested in the tidal effects, it is convenient to set the central object in system II as a black hole (with the same mass as the compact star), while keeping the compact star in system I. Then the energy reads

$$E_{\text{tot}} = C_{\omega} \frac{\partial(\theta_{\text{CS}} - \theta_{\text{BH}})}{\partial\omega} |A_{\text{in}}|^2. \quad (53)$$

Note we have omitted the subscript “t” in A_{in} .

It is important to emphasize that the energy here refers to the total energy difference, which includes not only the internal kinetic and potential energy of the compact star (similar to the term $\dot{Q}_L \dot{Q}^L + \omega_n^2 Q_L Q^L$ in its Newtonian counterpart), as well as the coupling energy between the multipole moments of the compact star and the tidal field (similar to the term $Q_L E^L$ in its Newtonian counterpart), but also the energy of the perturbed spacetime (GW) itself.

We also perform a consistency check of the energy expression Eq. (53) by comparing it with the Hamiltonian of the perturbation derived in Refs. [32, 33]. The details of

the Hamiltonian formalism are presented in Appendix E. In Fig. 5 we present a representative example, where both the compact star and the black hole are set to $M = 1.4 M_{\odot}$, and the compactness of the compact star is chosen to be $\mathcal{C} = 0.15$. We compare the total energy E_{tot} , calculated by the flux balance method [Eq. (53)], with the Hamiltonian difference $\mathcal{H} = \mathcal{H}_{\text{CS}} - \mathcal{H}_{\text{BH}}$, obtained from the Hamiltonian formalism. The excellent agreement between the two confirms the consistency of the two methods.

In this subsection, we have derived the total energy E_{tot} of the spacetime under steady driving, established its connection to the scattering coefficient (i.e., $E_{\text{tot}} \propto \partial\theta/\partial\omega$), and confirmed the result numerically using the Hamiltonian formalism. Although this discussion is of physical interest and provides valuable insight into the wave scattering picture, E_{tot} is not the quantity we ultimately seek—namely, the star’s tidal binding energy E_{tid} . As discussed above, E_{tot} includes not only the star’s tidal energy, but also the energy carried by the driving field. This distinction is clearly illustrated in Fig. 5, where we also compare E_{tot} with the tidal energy E_{tid} calculated in the next subsection. As expected, $E_{\text{tot}} \neq E_{\text{tid}}$.

Therefore, in Sec. IV B, we will employ a self-force approach to compute the tidal energy of the star in the extreme mass ratio limit. We then further rescale this result to comparable-mass systems in Sec. IV C, using the EOB framework.

B. Equilibrium tidal energy in the extreme mass ratio limit

We now focus on the computation of the tidal energy, which enters the binary equation of motion. Motivated by the duality between the wave-scattering problem and the point-mass scenario discussed in Sec. II, we compute the energy of a point mass orbiting a compact star, following a self-force approach similar to that of Ref. [34]. Below we briefly summarize the basic strategy; the detailed formalism is presented in Appendix C.

The metric of a point particle m_2 orbiting the compact star m_1 with $m_2 \ll m_1$ can be written as

$$g_{ab} = g_{ab}^0 + h_{ab}, \quad (54)$$

where g_{ab}^0 is the metric of the static background spacetime and h_{ab} is the metric perturbation. Without loss of generality, we consider that the circular orbit of the point mass is confined to the equatorial plane, $x^a(\tau) = [t(\tau), r_0, \theta_0 = \frac{\pi}{2}, \phi(\tau)]$. We then solve the metric perturbation in Regge-Wheeler gauge. With the perturbations at hand, we can locally define a mechanical binding energy based on the first law of binary mechanics (FLBM) [46, 47], which expresses the binding energy in terms of the first-order Detweiler redshift z_{SF} [48],

$$E_{\text{SF}} = \frac{1}{2} z_{\text{SF}} - \frac{y}{3} \frac{dz_{\text{SF}}}{dy} - 1 + \sqrt{1 - 3y} + \frac{y}{6} \frac{5 - 12y}{(1 - 3y)^{3/2}}, \quad (55)$$

where

$$z_{\text{SF}} = -(1 - 3y)^{1/2} \frac{1}{2} \bar{u}_a \bar{u}_b h_{ab}^{\text{R}}, \quad (56)$$

is gauge-invariant and $y \equiv (m_1 \Omega)^{2/3}$. Here \bar{u}^a is the non-radial part of the four-velocity of the particle with no h_{ab} terms. h_{ab}^{R} denotes the regular part of the metric perturbation. Note that in our case, the Detweiler redshift can be decomposed into two parts:

$$z_{\text{SF}} = z_{\text{SF,BH}} + z_{\text{SF,tid}}, \quad (57)$$

where the first term, $z_{\text{SF,BH}}$, corresponds to self-force contribution in binary black hole systems, while the second term, $z_{\text{SF,tid}}$, encapsulates the tidal effects arising from the compact star. The self-force contribution $z_{\text{SF,BH}}$ has been extensively studied in the literature [47, 48]. In this work, we focus on the tidal contribution, $z_{\text{SF,tid}}$, which can be expressed as

$$z_{\text{SF,tid}} = -(1 - 3y)^{1/2} \frac{1}{2} \bar{u}_a \bar{u}_b (h_{ab}^{\text{CS}} - h_{ab}^{\text{BH}}). \quad (58)$$

Since the singular parts of h_{ab}^{CS} and h_{ab}^{BH} are identical in our setup, no regularization of h_{ab} is needed. It is important to note that in SF calculations, the redshift is viewed as an expansion in the mass ratio $q \equiv m_2/m_1$, evaluated at fixed y . For comparison with PN and EOB results, it is convenient to switch to the standard dimensionless invariant PN parameter, $x \equiv [(m_1 + m_2)\Omega]^{2/3}$. In terms of x , the Detweiler redshift at linear order in the symmetric mass ratio $\nu \equiv m_1 m_2 / (m_1 + m_2)^2$ becomes

$$z(x) = \frac{x}{\sqrt{1 - 3x}} + z_{\text{SF,BH}}(x) + z_{\text{SF,tid}}(x). \quad (59)$$

We derive in Appendix D the analytic solution of the $(\ell, m) = (2, 0)$ mode contribution to the Detweiler redshift [Eq. (D10)], denoted as $z_{\text{SF,tid}}^{20}$. The contributions from the $(\ell, m) = (2, \pm 2)$ modes, $z_{\text{SF,tid}}^{22}$, can be obtained numerically. In what follows, we provide an analytic representation of the numerical data in the following form:

$$z_{\text{SF,tid}}^{22}(x) = z_{\text{SF,tid}}^{20} \frac{\omega_f^2}{\omega_f^2 - 4\Omega^2} (\alpha_0 + \alpha_1 x + \alpha_2 x^2 + \alpha_3 x^3 + \alpha_4 x^4 + \alpha_5 x^5 + \alpha_6 x^6), \quad (60)$$

with $\alpha_0 = 3/2$, which captures both the asymptotic behavior $z_{\text{SF,tid}}^{22} \rightarrow \frac{3}{2} z_{\text{SF,tid}}^{20}$ at $x \rightarrow 0$, and the resonance feature at $2\Omega \rightarrow \omega_f$. The coefficients are found to be $\alpha_1 = -6.005$ and $\alpha_2 = 21.94$, with uncertainty in the last digit. Therefore, in the following, we fix $\alpha_1 = -6$ and $\alpha_2 = 22$, while all other coefficients α_i ($i \geq 3$) are obtained by fitting to numerical data. The optimal coefficients are found to be

$$\alpha_3 = -60.18736362, \quad (61a)$$

$$\alpha_4 = -635.63344683, \quad (61b)$$

$$\alpha_5 = 5931.89992854, \quad (61c)$$

$$\alpha_6 = -18416.0079901. \quad (61d)$$

C. Effective-one-body approach

In this subsection, we implement the tidal contribution of the self-force into the EOB formalism, following the approach first introduced in Ref. [49]. Within the EOB framework, the two-body dynamics of non-spinning compact objects is described by mapping the real Hamiltonian H_{EOB} to an effective Hamiltonian H_{eff} , which corresponds to a test particle of mass $\mu = \frac{m_1 m_2}{m_1 + m_2}$ moving in a deformed Schwarzschild background with total mass $M = m_1 + m_2$, via [50]

$$H_{\text{EOB}} = M \sqrt{1 + 2\nu \left(\frac{H_{\text{eff}}}{\mu} - 1 \right)}. \quad (62)$$

The EOB effective metric reads

$$g_{ab}^{\text{eff}} dx^a dx^b = -A(r) dt^2 + B(r) dr^2 + r^2 d\Omega^2, \quad (63)$$

together with the mass-shell constraint [51]

$$g_{\text{eff}}^{ab} p_a p_b + \mu^2 + Q = 0. \quad (64)$$

Here, the potential Q encodes possible effective interactions that lead to a non-geodesic motion. The effective Hamiltonian is given by

$$H_{\text{eff}}^2 = A(\mu^2 + B^{-1} p_r^2 + p_\phi^2 u^2 + Q). \quad (65)$$

It is convenient to work in the DJS gauge [51], in which Q depends only on the radial momentum p_r , such that $Q = 0$ for the circular orbits considered in this work. The EOB potential $A(r)$ can be written as [49–51]

$$A(u) = A_{\text{pm}}(u) + A_{\text{tid}}(u), \quad (66)$$

$$A_{\text{pm}}(u) = 1 - 2u + 2\nu u^3 + \left(\frac{94}{3} - \frac{41}{32} \pi^2 \right) \nu u^4, \quad (67)$$

where $u \equiv M/r$ denotes the inverse Schwarzschild-like EOB radial coordinate. With the potential $A(u)$ at hand, we can compute the circular-orbit EOB energy as

$$E_{\text{EOB}}(u) = M \sqrt{1 + 2\nu \left(\frac{E_{\text{eff}}}{\mu} - 1 \right)}, \quad (68)$$

$$E_{\text{eff}}(u) = \mu \sqrt{\frac{2A^2(u)}{2A(u) + uA'(u)}}. \quad (69)$$

By computing the difference between EOB energy with and without the tidal contribution A_{tid} , we can obtain the tidal energy as function of orbit frequency Ω ,

$$E_{\text{tid}}(\Omega) = E_{\text{EOB}}(\Omega; A = A_{\text{pm}} + A_{\text{tid}}) - E_{\text{EOB}}(\Omega; A = A_{\text{pm}}), \quad (70)$$

where

$$\Omega = \frac{\partial H_{\text{EOB}}}{\partial p_\phi}. \quad (71)$$

In our self-force formalism, the tidal contribution to the EOB potential, $A_{\text{tid}}(u)$, is found to be related to the redshift function via [49]

$$A_{\text{SF,tid}}(u) = \nu z_{\text{SF,tid}}(u) \sqrt{1 - 3u} + \mathcal{O}(\nu^2). \quad (72)$$

Although our current analysis is restricted to linear order in ν , we are able to determine all PN corrections at this order (see, e.g. Fig. 6). On the other hand, the tidal contribution can also be derived from an effective-action approach. In the adiabatic-tide limit (AT), the tidal part of $A(u)$ can be expressed up to 2PN order as [52]

$$A_{2\text{PN,AT}} = -\frac{3\lambda X_2 u^6}{X_1 M^5} \left[1 + \frac{5}{2} X_1 u + \left(\frac{337}{28} X_1^2 + \frac{1}{8} X_1 + 3 \right) u^2 + \mathcal{O}(u^3) \right], \quad (73)$$

where $X_1 = m_1/M$ and $X_2 = m_2/M$. λ is the tidal deformability. It is worth noting that our self-force expression, Eq. (72), agrees with Eq. (73) at 2PN order. To see this, we plug Eq. (D10) and Eq. (60) into $z_{\text{SF,tid}} = z_{\text{SF,tid}}^{20} + 2z_{\text{SF,tid}}^{22}$ and take the adiabatic limit. This yields

$$A_{\text{SF,AT}} = -\frac{3\lambda X_2 u^6}{M^5} \left[1 + \frac{5}{2} u + \frac{849}{56} u^2 + \mathcal{O}(u^3) \right], \quad (74)$$

which is in exact agreement with Eq. (73) when taking $X_1 \rightarrow 1$. To capture the dynamic tidal effects, Ref. [2] suggests an effective approach by replacing the static tidal deformability λ in Eq. (73) with λ_{eff} , i.e.,

$$A_{2\text{PN,DT}} = -\frac{3\lambda_{\text{eff}} X_2 u^6}{X_1 M^5} \left[1 + \frac{5}{2} X_1 u + \left(\frac{337}{28} X_1^2 + \frac{1}{8} X_1 + 3 \right) u^2 + \mathcal{O}(u^3) \right], \quad (75)$$

where

$$\lambda_{\text{eff}} = \frac{\lambda}{4} + \frac{3\lambda}{4} \frac{\omega_f^2}{\omega_f^2 - 4\Omega^2}. \quad (76)$$

We now have two independent expressions for the tidal part of the EOB potential, A_{tid} , given by Eq. (72) and Eq. (75), both of which can be expanded as series in X_2 and u , as illustrated in Fig. 6. Inspired by Ref. [53], we propose to construct a hybrid tidal potential, which combines information from both approaches,

$$A_{\text{tid}} = A_{\text{SF,tid}} + A_{2\text{PN,DT}} - A_{\text{ovp}}, \quad (77)$$

where

$$A_{\text{ovp}} = -\frac{3\lambda_{\text{eff}} X_2 u^6}{M^5} \left(1 + \frac{5}{2} u + \frac{849}{56} u^2 \right) \quad (78)$$

denotes the contribution from the overlap regime as shown in Fig. 6.

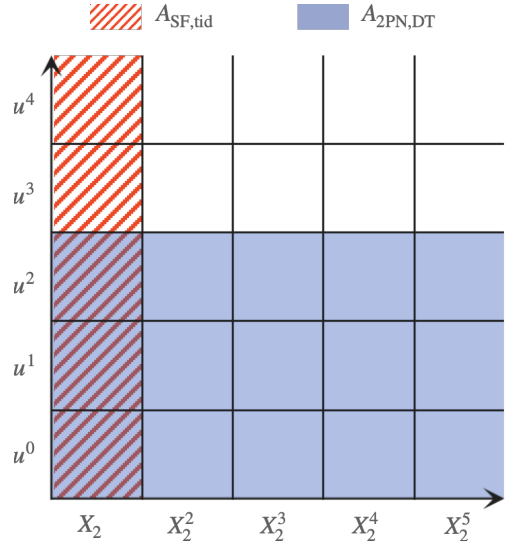


Figure 6. Schematic illustration of $A_{\text{SF,tid}}$ and $A_{2\text{PN,DT}}$ as functions expanded in terms of X_2 and u . The overlapping region, A_{ovp} , corresponds to the intersection between the red slanted lines and the blue shaded area.

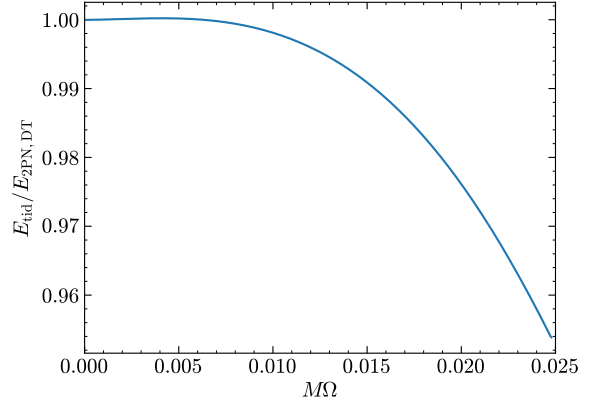


Figure 7. Ratio of tidal energy computed using A_{tid} and $A_{2\text{PN,DT}}$ in the extreme mass-ratio limit ($m_2 \ll m_1$). The stellar model is constructed from a polytropic equation of state with $n = 1$, and fixed to $M = m_1 = 1.4 M_\odot$ and $\mathcal{C} = 0.15$.

D. Results

In Fig. 7 and Fig. 8, we compare the tidal energy computed from A_{tid} and $A_{2\text{PN,DT}}$ in the extreme mass-ratio limit and in the equal-mass case, respectively. The compact star is constructed from a polytropic equation of state with $n = 1$, and fixed to $m_1 = 1.4 M_\odot$ and $\mathcal{C} = 0.15$ ($R = 13.83$ km), corresponding to a dimensionless tidal deformability $\Lambda_1 \equiv \lambda/m_1^5 = 715$. In both cases, we find that incorporating self-force corrections leads to a $\sim 3\%$ correction in the tidal energy at a GW frequency of $f_{\text{GW}} = \Omega/\pi = 1000$ Hz.

To calculate the GW phase difference accumulated during the inspiral stage, we adopt the following approxi-

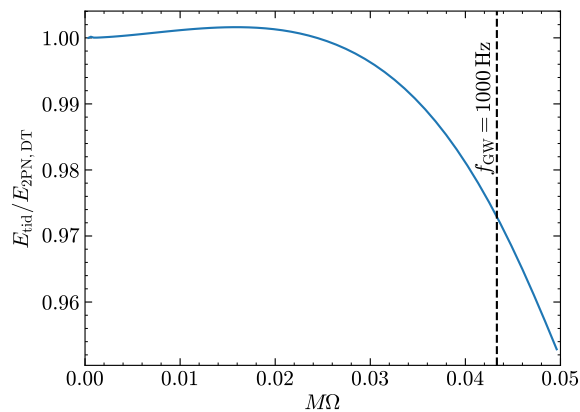


Figure 8. Same as Fig. 7, but for an equal-mass binary ($M = m_1 + m_2 = 2.8 M_\odot$). The dashed line indicates the GW frequency of $f_{\text{GW}} = \Omega/\pi = 1000$ Hz.

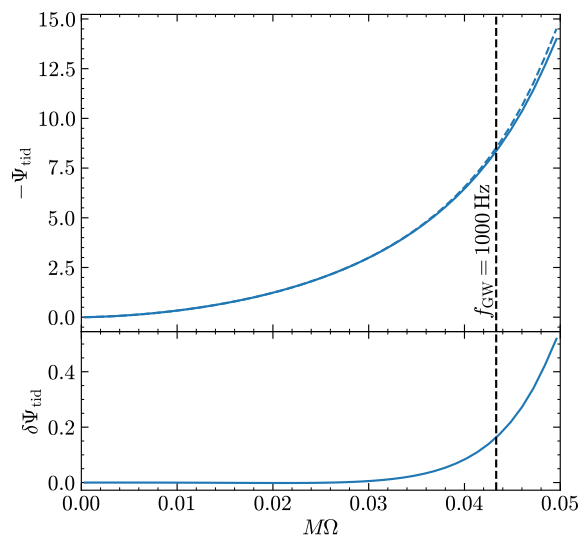


Figure 9. Upper: Accumulated tidal phase computed using A_{tid} (solid line) and $A_{2\text{PN,DT}}$ (dashed) for the equal-mass binary case as shown in Fig. 8. Lower: The phase difference between the two models.

mation

$$\frac{d\Psi_{\text{tid}}}{d\Omega} = 2\Omega \frac{dE_{\text{tid}}/d\Omega}{\dot{E}}, \quad (79)$$

where

$$\dot{E} = -\frac{32}{5} M^{4/3} \mu^2 \Omega^{10/3}. \quad (80)$$

In Fig. 9, we show the accumulated tidal phase obtained using A_{tid} model and $A_{2\text{PN,DT}}$ model. It can be seen that incorporating self-force corrections leads to a phase modulation reaching approximately 0.2 radian at $f_{\text{GW}} \sim 10^3$ Hz, and over 0.5 radian before the merger.

V. CONCLUSION

In this work, we study the excitation of compact stars under external tidal fields in the fully relativistic regime. This problem has been studied in the Newtonian regime in the past, where the external tidal forces can be decomposed into a mode basis and the star oscillations can be effectively described by the evolution of a set of modes. For relativistic stars, this framework no longer holds because the quasi-normal modes of the star do not form a complete basis for star perturbations, nor is an orthogonal projection of modes known.

We find that the scattering wave formalism becomes particularly useful in studying this relativistic problem. First, it can be shown that a system with a point mass orbiting around the star can be mapped to another system with purely input and output waves. The scattering formulation naturally provides a gauge-invariant way to measure the strength of the external tidal field, which can be quantified by the amplitude of the ingoing wave in the equivalent scattering problem. Second, we have shown that the response function defined in the scattering formulation encodes critical information about the tidal response of the star. For example, the poles of the response function correspond to quasi-normal modes of the star, and the residue of poles has a direct analogy with the *black hole excitation factor* in black hole perturbation theory [31], which measures the susceptibility of modes to external drivings. It turns out that the residue W_n is approximately by the decay rate of the particular mode. In the equilibrium tide scenario, the phase of the response is intimately related to the total tidal energy within the spacetime, including both the fluid and gravitational perturbations.

With a time-dependent external tidal field, a set of modes may be transiently excited if the tidal field frequency crosses the mode frequency at certain times. We are able to compute the energy of the transiently excited modes during this process, which is proportional to $|W_n|$ and the square of the amplitude of the external tidal field. The relativistic formula agrees with the Newtonian formula in the low-frequency, weak-gravity regime, but differs significantly for compact stars. For example, for a $1.4 M_\odot$ neutron star with radius ~ 13 km, if a g_1 -mode is resonantly excited, the Newtonian formula may over-predict the mode energy by a factor of ten. This large discrepancy calls for necessary re-examination of previous resonant mode calculation for various kinds of modes. Implementing Eq. (36) may have a dramatic impact on the predictions.

The $\ell = 2$ f-mode represents the dominant contribution of equilibrium tide in inspiraling binary neutron star systems. Because the f-mode frequency is generally larger than the merger frequency, these modes are not expected to be on resonance in the inspiral stage. Within the scattering formalism, through a flux-balance calculation, we can prove that the tidal energy in spacetime is proportional to $\partial\theta/\partial\omega$, where θ is the phase of the response

function. This formula is numerically checked with the Hamiltonian formula of perturbed stars derived by Moncrief in [32, 33]. However, this tidal energy cannot be directly used to compute the tidal binding energy of a binary neutron star system, as part of the energy computed in the scattering formalism belongs to the freely propagating waves.

In order to compute the tidal energy of a binary star system in the relativistic regime, we study the model problem with a point mass orbiting around a star. The tidal response of the star formally appears at the same order as the gravitational self force of the point mass in the expansion of the mass ratio. In particular, in order to account for the tidal energy of the binary, it is best to compute the gravitational field at infinity to extract the ADM mass of the whole system, which formally requires gravitational perturbations to the sub-leading order in mass-ratio (the same order as the second-order self force). Fortunately according to the discussion in [46], one can apply the first law of binary mechanics to obtain a canonical energy that only depends on the first-order gravitational perturbation in the near-zone. For the black hole case the definition with canonical energy agrees with the definition using ADM mass within 10^{-5} fractional difference [54]. Therefore we also apply this definition of canonical energy to approximate the tidal energy of a star binary. In the extreme mass ratio limit, this energy differs the effective-one-mode energy that has been widely adopted in literature by up to 3% at $f_{\text{GW}} \sim 10^3$ Hz. Adopting an Effective-One-Body formalism to scale this canonical energy for comparable mass-ratio systems, we find that the resulting phase modulation for binary neutron stars can reach 0.2 rad at 10^3 Hz and ≥ 0.5 rad before merger. Note that the phase modulation only includes the relativistic correction on the tidal energy, but there is also possibly a correction on the tidal flux. Together the phase modulation may be significant, so that this new relativistic treatment of tidal energy should be incorporated into future waveforms of neutron star binaries.

As the binary enters the late inspiral stage, the excitation of stars may receive additional contributions beyond the equilibrium-tide prediction, e.g. the terms following the first term in Eq. (6.50) of Ref. [2]. These terms directly correspond to “free oscillations” of the star upon full excitation of the mode across the resonance. According to the analysis in Sec. III, the relativistic energy correction of transiently excited f-modes may be greater than 50%. Even if the f-mode is not fully excited in the inspiral stage, the relativistic correction for this part of the contribution can still be significant. It is also important to note that the calculations in Sec. IV B assume an equilibrium tide scenario, so that they are not directly applicable to describe non-steady effects. However, it may be instructive to explore the scenario with a point mass orbiting around a star following an inspiralling orbit, which may be mapped to these systems with non-equilibrium tides. This study is beyond the scope of this work.

VI. ACKNOWLEDGEMENTS

We are grateful to Zihan Zhou for answering questions about scattering amplitude calculations of neutron star tides and Sizheng Ma for discussions about the scattering formalism. We thank Eric Poisson for many useful comments on the manuscript. ZM is supported by the Postdoctoral Innovation Talent Support Program of CPSF (No. BX20240223) and CPSF funded project (No. 2024M761948).

Appendix A: Perturbation of relativistic stars

In this Appendix, we describe the technical details involved in the calculation of perturbation of relativistic stars.

1. Static background spacetime

For a non-rotating star, the static and spherically symmetric line element is given by

$$ds^2 = g_{ab}dx^a dx^b = -e^{2\nu} dt^2 + e^{2\lambda} dr^2 + r^2(d\theta^2 + \sin^2\theta d\phi^2), \quad (\text{A1})$$

where the metric components ν and λ are functions of r only. We model the star as a perfect fluid, with the stress-energy-momentum tensor given by

$$T^{ab} = (p + \varepsilon)u^a u^b + pg^{ab}, \quad (\text{A2})$$

where u^a is the four-velocity. p and ε denote the pressure and energy density, respectively, which are connected via an equation of state $p = p(\varepsilon)$. The Einstein field equations for this system reduce to the Tolman–Oppenheimer–Volkoff (TOV) equations, expressed as

$$\frac{dm}{dr} = 4\pi r^2 \varepsilon, \quad (\text{A3})$$

$$\frac{dp}{dr} = -\frac{(p + \varepsilon)(m + 4\pi r^2 p)}{r(r - 2m)}, \quad (\text{A4})$$

$$\frac{d\nu}{dr} = \frac{m + 4\pi r^2 p}{r(r - 2m)}. \quad (\text{A5})$$

where $m(r)$ is defined as

$$m(r) = \frac{r}{2} \left[1 - e^{-2\lambda(r)} \right]. \quad (\text{A6})$$

Given the central pressure p_0 (or energy density ε_0) at $r = 0$, Eqs. (A3–A5) can be integrated outward the pressure vanishes, i.e., $p(R) = 0$. This determines the stellar radius R , and the corresponding gravitational mass $M = m(R)$. Note there is an arbitrary constant in the function ν , which can be fixed by requiring

$$\nu(R) = -\lambda(R) = \frac{1}{2} \ln \left(1 - \frac{2M}{R} \right). \quad (\text{A7})$$

2. Perturbations inside the star

In this work we only consider the even-parity perturbations. We write the metric perturbation in Regge-Wheeler gauge as [35, 55]

$$h_{ab} = [\zeta^\ell H_0 e^{2\nu} dt^2 + 2i\omega r \zeta^\ell H_1 dt dr + \zeta^\ell H_0 e^{2\lambda} dr^2 + \zeta^\ell K r^2 (d\theta^2 + \sin^2 \theta d\phi^2)] Y_{\ell m}(\theta, \phi) e^{-i\omega t}, \quad (\text{A8})$$

with

$$\zeta = \begin{cases} r/R, & 0 \leq r < R, \\ 1, & r \geq R, \end{cases} \quad (\text{A9})$$

and $Y_{\ell m}(\theta, \phi)$ the spherical harmonics. We also write the fluid displacement as

$$\xi^r = \zeta^\ell r^{-1} e^{-\lambda} W Y_{\ell m} e^{-i\omega t}, \quad (\text{A10})$$

$$\xi^\theta = -\zeta^\ell r^{-2} V \partial_\theta Y_{\ell m} e^{-i\omega t}, \quad (\text{A11})$$

$$\xi^\phi = -\zeta^\ell r^{-2} \sin^{-2} \theta V \partial_\phi Y_{\ell m} e^{-i\omega t}. \quad (\text{A12})$$

The Eulerian perturbations of energy density and pressure are given by

$$\delta\varepsilon = (p + \varepsilon) \frac{\Delta n}{n} - \xi^i \frac{d\varepsilon}{dx^i}, \quad (\text{A13})$$

$$\delta p = \Gamma p \frac{\Delta n}{n} - \xi^i \frac{dp}{dx^i}, \quad (\text{A14})$$

where $\Gamma = [(p + \varepsilon)/p](\partial p/\partial\varepsilon)_s$ is the adiabatic index. The Lagrangian perturbation of the baryon number density Δn can be derived from the baryon number conservation $\nabla_\mu(nu^\mu) = 0$, it reads

$$\Delta n = -n \nabla_i \xi^i - \frac{1}{2} n \delta g^{(3)}/g^{(3)}, \quad (\text{A15})$$

with $g^{(3)}$ the determinant of the metric of the 3-geometry at constant time. Plugging these perturbations [Eqs. (A8-A14)] into linear Einstein equation $\delta G_{\mu\nu} = 8\pi \delta T_{\mu\nu}$, we get [55]

$$H'_1 = \left(\lambda' - \nu' - \frac{\ell+1}{r} \right) H_1 - \frac{e^{2\lambda}}{r} [H_0 + K + 16\pi(p + \varepsilon)V], \quad (\text{A16})$$

$$K' = \left(\nu' - \frac{\ell+1}{r} \right) K + \frac{1}{r} H_0 - \frac{\ell(\ell+1)}{2r} H_1 + 8\pi(p + \varepsilon) \frac{e^\lambda}{r} W, \quad (\text{A17})$$

$$W' = -\frac{\ell+1}{r} W + r e^\lambda \left[\frac{e^{-\nu}}{\Gamma p} X - \frac{\ell(\ell+1)}{r^2} V - \frac{1}{2} H_0 - K \right], \quad (\text{A18})$$

$$X' = -\frac{\ell}{r} X + (p + \varepsilon) e^\nu \left\{ \left(\frac{\nu'}{2} - \frac{1}{2r} \right) H_0 + \left(\frac{1}{2r} - \frac{3\nu'}{2} \right) K + \left[\frac{1}{2} \omega^2 r e^{-2\nu} + \frac{\ell(\ell+1)}{4r} \right] H_1 - \frac{\ell(\ell+1)}{r^2} \nu' V - \frac{1}{r} \left[\omega^2 e^{\lambda-2\nu} + 4\pi(p + \varepsilon) e^\lambda - r^2 \left(\frac{e^{-\lambda}}{r^2} \nu' \right)' \right] W \right\}, \quad (\text{A19})$$

with

$$H_0 = \left\{ -8\pi r^2 e^{-\nu} X - \left[\omega^2 r^2 e^{-2\nu} - \frac{1}{2}(\ell-1)(\ell+2) + r^2 e^{-2\lambda} \left(\nu'^2 - \frac{\nu'}{r} \right) \right] K - e^{-2\lambda} \left[\omega^2 r^2 e^{-2\nu} - \frac{1}{2} \ell(\ell+1) r \nu' \right] H_1 \right\} \left[(r\nu' - 1) e^{-2\lambda} + \frac{1}{2} \ell(\ell+1) \right]^{-1}, \quad (\text{A20})$$

$$X = \omega^2 (p + \varepsilon) e^{-\nu} V - \frac{e^{\nu-\lambda}}{r} p' W - \frac{1}{2} (p + \varepsilon) e^\nu H_0, \quad (\text{A21})$$

where a prime denotes differentiation with respect to r . At the center of the star ($r = 0$), all perturbation functions

must be regular, leading to the boundary conditions,

$$X(0) = (p_0 + \varepsilon_0) e^{\nu(0)} \left\{ \left[\frac{4\pi}{3} (\varepsilon_0 + 3p_0) \right. \right.$$

$$\left. -\frac{\omega^2 e^{-2\nu(0)}}{\ell} \right] W(0) - \frac{1}{2} K(0) \Big\}, \quad (\text{A22})$$

$$H_1(0) = \frac{-2\ell K(0) + 16\pi(p_0 + \varepsilon_0)W(0)}{\ell(\ell + 1)}. \quad (\text{A23})$$

At the star surface ($r = R$), the Lagrangian pressure variation must vanish, imposing another boundary condition as

$$X(R) = 0. \quad (\text{A24})$$

At this point, we have four equations [Eqs. (A16–A19)] governing the radial evolution of four independent variables (H_1, K, W, X), along with three constraint equations [Eqs. (A22–A24)]. This leaves one remaining degree of freedom, which, as we will see, can be determined by the gravitational perturbation in the exterior spacetime of the star.

3. Perturbations outside the star

Outside the star, only gravitational perturbations are relevant, where the system of perturbation equations [Eqs. (A16–A19)] reduce to a second-order wave function [36]

$$\frac{d^2 Z}{dr_*^2} + (\omega^2 - V_Z)Z = 0, \quad (\text{A25})$$

with the effective potential given by

$$V_Z = \frac{e^{-2\lambda} [2n^2(n+1)r^3 + 6n^2Mr^2 + 18nM^2r + 18M^3]}{r^3(nr + 3M)^2}. \quad (\text{A26})$$

Here $n = (\ell - 1)(\ell + 2)/2$ and the tortoise coordinate r_* is defined as

$$\frac{d}{dr_*} = e^{\nu-\lambda} \frac{d}{dr}. \quad (\text{A27})$$

The master variable Z is related to the metric perturbation functions as

$$\begin{aligned} Z(r_*) &= \frac{r^2}{nr + 3M} e^{-2\lambda} H_1 + \frac{r^2}{nr + 3M} K, \quad (\text{A28}) \\ \frac{dZ(r_*)}{dr_*} &= -\frac{n(n+1)r^2 + 3nMr + 6M^2}{(nr + 3M)^2} e^{-2\lambda} H_1 \\ &\quad - \frac{nr^2 - 3nMr - 3M^2}{(nr + 3M)^2} K. \quad (\text{A29}) \end{aligned}$$

On the surface of the star, it must match the internal solutions of $H_1(R)$ and $K(R)$ obtained by solving Eqs. (A16–A19).

Eq. (A25) admits two linearly independent solutions with the following asymptotic behavior at large r ,

$$Z_{\text{out}} = e^{i\omega r_*} [1 + a_1 r^{-1} + a_2 r^{-2} + a_3 r^{-3} + \mathcal{O}(r^{-4})], \quad (\text{A30})$$

$$Z_{\text{in}} = e^{-i\omega r_*} [1 + a_1^* r^{-1} + a_2^* r^{-2} + a_3^* r^{-3} + \mathcal{O}(r^{-4})], \quad (\text{A31})$$

which corresponds to the outgoing and ingoing wave, respectively. The coefficients a_j and their complex conjugates a_j^* are given by

$$a_1 = \frac{i(n+1)}{\omega}, \quad (\text{A32})$$

$$a_2 = -\frac{1}{2\omega^2} \left[n(n+1) + \frac{3i(n+2)}{n} M\omega \right], \quad (\text{A33})$$

$$\begin{aligned} a_3 &= -\frac{i}{6\omega^3} \left[n(n-2)(n+1) + 3i(n+4)M\omega \right. \\ &\quad \left. - \frac{18(2n+3)}{n^2} M^2\omega^2 \right]. \quad (\text{A34}) \end{aligned}$$

The general solution to Eq. (A25) can be expressed as

$$Z = A_{\text{out}} Z_{\text{out}} + A_{\text{in}} Z_{\text{in}}. \quad (\text{A35})$$

The coefficients A_{out} and A_{in} represent the amplitudes of the outgoing and ingoing waves, respectively. To obtain A_{out} and A_{in} , we directly integrate Eq. (A25) and then match the results to Eq. (A35) with the asymptotic expansion in Eqs. (A30 & A31) at large r . In practice, we set $r = 300/\omega$ to achieve a relatively high precision solution.

Appendix B: Computing the poles of \mathcal{R} and the corresponding residue W_n

Given any frequency ω , the ingoing and outgoing amplitudes A_{in} and A_{out} can be obtained using the method presented in Appendix A, which enables us to compute the scattering/reflection coefficient

$$\mathcal{R}(\omega) = \frac{A_{\text{out}}}{A_{\text{in}}}. \quad (\text{B1})$$

The function $\mathcal{R}(\omega)$ possesses series poles in the complex frequency plane, which correspond to the quasi-normal modes of the star. To compute these poles, we proceed as follows:

1. We first search along the real axis to obtain an approximate value of the real part of the mode frequency, ω_{nR}^1 , following the method described in Ref. [55].
2. We then search along the imaginary axis to find the frequency $\omega_{nR}^1 + i\gamma_n^1$ that maximizes $|\mathcal{R}|$.
3. Next, we search again along the real axis for the frequency $\omega_{nR}^2 + i\gamma_n^1$ that maximizes $|\mathcal{R}|$.
4. Steps 2 and 3 are repeated iteratively until the desired precision for the frequency is achieved.

In the actual calculation, the internal solution of the perturbation contains numerical errors arising from interpolation errors in the background star model. These errors can affect the precise determination of \mathcal{R} . To overcome this issue, we first compute a set of $H_1(R, \omega)$ and $K(R, \omega)$ in a small interval $[\omega_{nR}^1 - \Delta\omega, \omega_{nR}^1 + \Delta\omega]$ at star surface $r = R$. We then use (5, 5) Padé approximation to fit these functions in this region, i.e.,

$$H_1(R, \tilde{\omega}) = \frac{A_0 + A_1\tilde{\omega} + A_2\tilde{\omega}^2 + A_3\tilde{\omega}^3 + A_4\tilde{\omega}^4 + A_5\tilde{\omega}^5}{B_0 + B_1\tilde{\omega} + B_2\tilde{\omega}^2 + B_3\tilde{\omega}^3 + B_4\tilde{\omega}^4 + B_5\tilde{\omega}^5} \quad (\text{B2})$$

$$K(R, \tilde{\omega}) = \frac{C_0 + C_1\tilde{\omega} + C_2\tilde{\omega}^2 + C_3\tilde{\omega}^3 + C_4\tilde{\omega}^4 + C_5\tilde{\omega}^5}{D_0 + D_1\tilde{\omega} + D_2\tilde{\omega}^2 + D_3\tilde{\omega}^3 + D_4\tilde{\omega}^4 + D_5\tilde{\omega}^5} \quad (\text{B3})$$

where $\tilde{\omega} = (\omega - \omega_{nR}^1)/\Delta\omega$. This allows us to ensure the smoothness of the internal solution at the star's surface, thereby reducing errors when solving for the external solution. With this method, we can achieve high precision in calculating the f-mode and g-mode frequencies (including their imaginary part).

Once the pole $\omega_n = \omega_{nR} + i\gamma_n$ is located, the residue W_n can be directly calculated as follows

$$W_n = \left[\frac{d}{d\omega} \left(\frac{1}{\mathcal{R}} \right) \right]^{-1} \Big|_{\omega=\omega_n}. \quad (\text{B4})$$

However, this method can be numerically challenging, as \mathcal{R} diverges near the pole, which can lead to significant loss of accuracy in the numerical differentiation. To overcome this difficulty, an alternative and numerically stable approach is to evaluate the residue via a contour integral around the pole. According to the residue theorem, the residue W_n at ω_n can be expressed as

$$W_n = \frac{1}{2\pi i} \oint_{\mathcal{C}} \mathcal{R}(\omega) d\omega, \quad (\text{B5})$$

where \mathcal{C} is a small closed contour enclosing the pole ω_n . This method avoids direct differentiation near a divergent point and is therefore less sensitive to numerical noise. In practice, \mathcal{C} can be taken as a small circle of radius ϵ around ω_n , and the integral can be approximated using the trapezoidal rule over the complex contour:

$$W_n \approx \frac{1}{2\pi i} \sum_{k=1}^N \mathcal{R}(\omega_k) \Delta\omega_k, \quad (\text{B6})$$

where $\omega_k = \omega_n + \epsilon e^{2\pi i k/N}$, and $\Delta\omega_k = \omega_{k+1} - \omega_k$. The value of ϵ should be small enough to stay within the linear regime, yet large enough to avoid floating-point round-off errors. In this work, we set $N = 20$ and $\epsilon = \gamma_n/5$ for our calculations. To test the numerical accuracy, we vary N to 30 or ϵ to $\gamma_n/10$, which results in a change of W_n by $\delta|W_n|/|W_n| \sim \mathcal{O}(10^{-5})$ for f-mode and $\sim \mathcal{O}(10^{-3})$ for g-mode. Therefore, we are confident that our results are accurate to this level.

Appendix C: Point mass orbiting around a compact star

In the point mass scenario, the perturbations are described in a manner similar to the formalism provided in Appendix A, with the only difference being that we have included the source term representing the point particle in the Zerilli equation, i.e., Eq. (A25) should be altered as

$$\frac{d^2 Z}{dr_*^2} + (\omega^2 - V_Z)Z = S. \quad (\text{C1})$$

In the case of a circular orbit in the equatorial plane, the source term is given by [37]

$$S = \frac{8\pi}{n+1} \mu \delta(\omega - m\Omega) e^{-2\lambda} \left(\frac{dA}{dr} + B \right) Y_{\ell m}^* \left(\frac{\pi}{2}, \phi \right), \quad (\text{C2})$$

where

$$A = \frac{r e^{-4\lambda}}{nr + 3M} \frac{1}{\sqrt{1 - 3M/r}} \delta(r - r_0), \quad (\text{C3})$$

$$B = - \frac{n(n+1)r^2 + 3nMr + 6M^2}{(nr + 3M)^2 r} \frac{e^{-2\lambda}}{\sqrt{1 - 3M/r}} \delta(r - r_0) - \frac{1}{n} \left[\frac{\ell(\ell+1)}{2} - m^2 \right] \frac{r\Omega^2}{\sqrt{1 - 3M/r}} \delta(r - r_0). \quad (\text{C4})$$

The general solution of Eq. (C1) can be expressed as

$$Z = \alpha Z_{\text{out}} + \beta Z_{\text{in}} + \int_{R_*}^{\infty} G(r_*, s_*) S(s_*) ds_*. \quad (\text{C5})$$

Here Z_{out} and Z_{in} are the two homogeneous solutions as in Eqs. (A30 & A31). α and β denote the amplitudes of the outgoing and ingoing waves, respectively, corresponding to the A_{out} and A_{in} used in the main text. $G(r_*, s_*)$ is the Green's function

$$G(r_*, s_*) = \frac{1}{W} \left[-Z_{\text{out}}(r_*) Z_{\text{in}}(s_*) + Z_{\text{in}}(r_*) Z_{\text{out}}(s_*) \right] \Theta(r_* - s_*), \quad (\text{C6})$$

where W is the Wronskian and $\Theta(x)$ is the Heaviside function. In the point mass scenario, there should be only outgoing wave at spatial infinity, which leading to the boundary condition

$$Z(r_*) \rightarrow \mathcal{A} e^{i\omega r_*}, \quad r \rightarrow \infty. \quad (\text{C7})$$

Appendix D: Analytic solution for $m = 0$ mode

For the $m = 0$ mode, we have $\omega = m\Omega = 0$, so the previous method of decomposing the solution into ingoing and outgoing parts no longer applies. Fortunately, we can calculate the analytic solution of perturbed metric functions in this situation. Here we focus only on the case

of $\ell = 2$, but our approach can be readily generalized to arbitrary $\ell \geq 3$. We begin with the $\omega = 0$ equation for H_0 , which reads [26]:

$$H_0'' + \left[\frac{2}{r} + e^{2\lambda} \left(\frac{2m}{r^2} + 4\pi r(p - \varepsilon) \right) \right] H_0' + \left[-\frac{6e^{2\lambda}}{r^2} + 4\pi e^{2\lambda} \left(5\varepsilon + 9p + \frac{\varepsilon + p}{dp/d\varepsilon} - 4\nu'^2 \right) \right] H_0 = S_H. \quad (\text{D1})$$

where S_H denotes a source term at $r = r_0$. Outside the star ($r > R$), Eq. (D1) reduces to

$$H_0'' + \left(\frac{2}{r} - 2\lambda' \right) H_0' - \left(\frac{6e^{2\lambda}}{r^2} + 4\lambda'^2 \right) H_0 = S_H. \quad (\text{D2})$$

We can write the exterior solution as

$$H_0 = \begin{cases} c_1 Q_2^2 \left(\frac{r}{M} - 1 \right) + c_2 P_2^2 \left(\frac{r}{M} - 1 \right), & R \leq r \leq r_0, \\ d_1 Q_2^2 \left(\frac{r}{M} - 1 \right), & r > r_0, \end{cases} \quad (\text{D3})$$

where P_2^2 and Q_2^2 are the associated Legendre functions. c_1 , c_2 and d_1 are coefficients to be determined. With H_0 known, we can obtain both K and H_1 , via

$$\begin{pmatrix} \frac{3M-r}{r(r-2M)} & -\frac{3}{r} \\ \frac{2r(r-2M)+M(r-3M)}{r(r-2M)} & \frac{3M}{r} \end{pmatrix} \begin{pmatrix} K \\ H_1 \end{pmatrix} = \begin{pmatrix} K' - \frac{1}{r} H_0 \\ \frac{2r+3M}{r} H_0 \end{pmatrix} \quad (\text{D4})$$

where $K' = H_0' + 2\nu' H_0$. Using Eq. (A28) and Eq. (A29) we get the solution of Z and dZ/dr^* .

For a compact star, we numerically integrate Eq. (D1) and match the interior solution of H_0 and H_0' to the exterior solution given in Eq. (D4), while for a black hole, we take $c_1 = 0$ and $c_2 = 1$. Now we are able to determine the ratio c_1/c_2 , which is related to the tidal deformability,

$$\frac{c_1}{c_2} = \frac{45}{8} \frac{\lambda}{M^5}. \quad (\text{D5})$$

The junction condition at $r = r_0$ can be read off from Eq. (C1),

$$[Z] = \frac{8\pi\mu}{3\sqrt{1-3M/r_0}} \frac{r_0 - 2M}{2r_0 + 3M} Y_{20}^* \left(\frac{\pi}{2}, \phi \right), \quad (\text{D6})$$

$$\left[\frac{dZ}{dr^*} \right] = \frac{8\pi\mu}{\sqrt{1-3M/r_0}} \frac{M^3 + 8M^2 r_0 + 4r_0^3}{2r_0^2(2r_0 + 3M)^2} Y_{20}^* \left(\frac{\pi}{2}, \phi \right). \quad (\text{D7})$$

Finally, we get the general solution for metric perturbations. For $R \leq r \leq r_0$, we have

$$H_0(r) = -\frac{\pi\mu}{6M^3 r_0 \sqrt{1-3M/r_0}} Y_{20}^* \left(\frac{\pi}{2}, \phi \right) \left[14M^3 - 12M^2 r_0 + 6M r_0^2 + (6M^3 - 12M^2 r_0 + 9M r_0^2 - 3r_0^3) \log \left(\frac{r_0}{r_0 - 2M} \right) \right] \left[\frac{c_1}{c_2} Q_2^2 \left(\frac{r}{M} - 1 \right) + P_2^2 \left(\frac{r}{M} - 1 \right) \right]. \quad (\text{D8})$$

Similarly, K can be obtained from H_0 via Eq. (D4), i.e.,

$$K(r) = \frac{r^2 - Mr - M^2}{r(r-2M)} H_0(r) + \frac{M}{2} H_0'(r). \quad (\text{D9})$$

Substituting Eq. (D8) and Eq. (D9) into Eq. (58), we get the analytical solution of Detweiler redshift for $(\ell, m) = (2, 0)$ mode. The result expanded to 7PN order is:

$$z_{\text{SF,tid}}^{20}(x) = -\frac{3\lambda x^6}{4M^5} \left(1 + 7x + \frac{226}{7} x^2 + \frac{872}{7} x^3 + \frac{257003}{588} x^4 + \frac{852697}{588} x^5 + \frac{30056977}{6468} x^6 + \frac{94191283}{6468} x^7 \right). \quad (\text{D10})$$

Appendix E: Hamiltonian formalism

In Ref. [32, 33] Moncrief developed a Hamiltonian description for the perturbations of a perfect fluid star, both

in the stellar interior and in the exterior Schwarzschild

spacetime,

$$\mathcal{H} = \mathcal{H}_I + \mathcal{H}_E. \quad (\text{E1})$$

For the fluid interior, the Hamiltonian is given by

$$\begin{aligned} 16\pi\mathcal{H}_I = & \int_0^R dr \left\{ e^{\nu-\lambda} \left[\frac{\ell(\ell+1)}{2(\ell-1)(\ell+2)} (\Lambda\pi_1 - 8\pi r^2 \varepsilon' \pi_2)^2 + 8\pi e^{-2\lambda} r^2 (p + \varepsilon) (\pi_1 - \pi_2')^2 \right. \right. \\ & \left. \left. + 8\pi r (p + \varepsilon) \ell(\ell+1) \pi_1 \pi_2 + 8\pi (p + \varepsilon) \ell(\ell+1) \pi_2'^2 \right] \right\} \\ & + \int_0^R dr \left\{ \frac{e^{\lambda+\nu}}{\Lambda^2} \left[\frac{(\ell-1)(\ell+2)}{2\ell(\ell+1)} e^{-2\lambda} (q_1 - q_2')^2 - \frac{(\ell-\ell)(\ell+2)}{2r} q_1 q_2 \right. \right. \\ & \left. \left. + \frac{(\ell-1)(\ell+2)}{2r^2 \Lambda} q_1^2 [(\ell-1)(\ell+2) - 8\pi r^3 \varepsilon'] + \frac{\partial p / \partial \varepsilon}{32\pi r^2 (p + \varepsilon)} (\Lambda q_2 + 8\pi r^2 \varepsilon' q_1)^2 \right] \right\} \\ & + \int_0^R dr \left\{ e^{\lambda+\nu} \left[\frac{\pi_4^2}{2\ell(\ell+1)} - 2e^{-2\lambda} \pi_4 (\pi_1 - \pi_2') - \frac{\ell(\ell+1) - \Lambda}{r} \pi_2 \pi_4 \right. \right. \\ & \left. \left. + \frac{2e^{-2\lambda}}{(\ell-1)\ell(\ell+1)(\ell+2)r^2} \pi_3^2 + \frac{2e^{-2\lambda}}{(\ell-1)(\ell+2)r^2} \pi_3 (r\Lambda\pi_1 + \pi_2(r\Lambda)') \right] \right\} \\ & + \int_0^R dr \left\{ \frac{e^{\nu-\lambda}}{8\pi r^2 (p + \varepsilon)} \left[\frac{1}{4} e^{2\lambda} \pi_4^2 + \frac{r^2}{\ell(\ell+1)} \left[\frac{1}{2} \pi_4' + \frac{\pi_4}{r} - \frac{\pi_3}{r^2} \right]^2 \right] \right\}, \end{aligned} \quad (\text{E2})$$

The variables q_1, \dots, q_4 and their conjugate momentum

π_1, \dots, π_4 are related to the metric perturbation functions as (in Regge-Wheeler gauge)

$$q_1 = \ell(\ell+1)rK - 2e^{-2\lambda}r(K - H_0 + rK' + r\lambda'K), \quad (\text{E3})$$

$$q_2 = e^{-2\lambda} \left\{ [2 + e^{2\lambda}\ell(\ell+1) - 4r\lambda'] H_0 + 2rH_0' + 2rK'(-3 + r\lambda') - 2r^2K'' \right. \quad (\text{E4})$$

$$\left. + [-2 + e^{2\lambda}\ell(\ell+1) + 4r^2\lambda'^2 - 2r^2\lambda''] K \right\}, \quad (\text{E5})$$

$$q_3 = q_4 = 0, \quad (\text{E6})$$

and

$$e^{\lambda+\nu}\pi_4 = -\ell(\ell+1)H_1 + 4r(\lambda' + \nu')e^{-2\lambda}H_1 + 2r[r\dot{K}' + (1 - r\nu')\dot{K} - \dot{H}_0], \quad (\text{E7})$$

$$\begin{aligned} e^{\lambda+\nu}\pi_3 = & e^{-2\lambda}r(6r\lambda' + 6r\nu' - 6r^2\lambda'^2 - 2r^2\nu'^2 - 8r^2\lambda'\nu' + 2r^2\lambda'' + 2r^2\nu'')H_1 \\ & + \ell(\ell+1)(r\lambda' - 1)rH_1 - \ell(\ell+1)r^2H_1' + 2r^3(\lambda' + \nu')e^{-2\lambda}H_1' \\ & + \frac{\ell(\ell+1)}{2}e^{2\lambda}r^2(\dot{H}_0 + \dot{K}) + (r\lambda' + r\nu' - 3)r^2\dot{H}_0 - (r\lambda' + 2r\nu' - 5)r^3\dot{K}' \\ & + (3 - 5r\nu' + r^2\nu'^2 - r\lambda' + r^2\lambda'\nu' - r^2\nu'')r^2\dot{K} - r^3\dot{H}_0' + r^4\dot{K}'' , \end{aligned} \quad (\text{E8})$$

$$\begin{aligned} e^{\lambda+\nu}\pi_2 = & \frac{2rH_1}{\Lambda} - \frac{4r^2e^{-2\lambda}}{\ell(\ell+1)\Lambda}(\lambda' + \nu')H_1 + \frac{2r^2}{\ell(\ell+1)\Lambda}\dot{H}_0 - \frac{2r^3}{\ell(\ell+1)\Lambda}\dot{K}' \\ & + \frac{2r^2(r\nu' - 1)}{\ell(\ell+1)\Lambda}\dot{K} - \frac{r^2e^{2\lambda}}{\Lambda}\dot{K}, \end{aligned} \quad (\text{E9})$$

$$\begin{aligned}
e^{\lambda+\nu}\pi_1 = & -\frac{2re^{-2\lambda}}{\ell(\ell+1)\Lambda^2}[(4\nu' - 6r\lambda'^2 - 2r\nu'^2 + 4\lambda' - 8r\lambda'\nu' + 2r\lambda'' + 2r\nu'')\Lambda \\
& + \ell(\ell+1)e^{2\lambda}(\Lambda' + \Lambda\lambda') - 2r(\lambda' + \nu')\Lambda']H_1 \\
& + \frac{2re^{-2\lambda}}{\ell(\ell+1)\Lambda}[\ell(\ell+1)e^{2\lambda} - 2r(\lambda' + \nu')]H_1' \\
& - \frac{r}{\ell(\ell+1)\Lambda^2}[\ell(\ell+1)e^{2\lambda}\Lambda + 2r(\lambda' + \nu')\Lambda - 4\Lambda + 2r\Lambda']\dot{H}_0 \\
& + \frac{r}{\ell(\ell+1)\Lambda^2}[(8r\nu' - 4 - 2r^2\nu'^2 + 2r\lambda' - 2r^2\lambda'\nu' + 2r^2\nu'')\Lambda \\
& + \ell(\ell+1)re^{2\lambda}\Lambda' + (2r - 2r^2\nu')\Lambda']\dot{K} \\
& + \frac{2r^2}{\ell(\ell+1)\Lambda}\dot{H}_0' + \frac{2r^2}{\ell(\ell+1)\Lambda^2}[(2r\nu' + r\lambda' - 4)\Lambda + r\Lambda']\dot{K}' - \frac{2r^3}{\ell(\ell+1)\Lambda}\dot{K}'', \tag{E10}
\end{aligned}$$

where

$$\Lambda = \ell(\ell+1) - 2e^{-2\lambda}(1+r\lambda'), \tag{E11}$$

and an overdot denotes differentiation with respect to t .

For the external Schwarzschild spacetime, we find that in the frequency domain considered in this work, the original Hamiltonian in Ref. [32] can be greatly simplified. The resulting expression is

$$\mathcal{H}_E = \frac{1}{64\pi} \frac{(\ell+2)!}{(\ell-1)!} \left\{ \int_{R_*}^{\infty} \omega^2 Z^2 dr_* + \left[\frac{Z\Lambda(Z\Lambda)_{r_*}}{2\Lambda^2} \right]_{R_*}^{\infty} \right\}. \tag{E12}$$

Here r_* is the tortoise coordinate and Z is the Zerilli variable.

Appendix F: An alternative way to compute W_n

1. Formalism

Let us first consider Regge-wheeler/Zerilli equation outside the star which is given by

$$\left(\frac{\partial^2}{\partial r_*^2} + \omega^2 - V(r) \right) \psi = 0, \tag{F1}$$

with matching condition at $r \rightarrow R$ and boundary condition at $r_* \rightarrow \infty$ as

$$\psi \rightarrow A_{\text{in}} e^{-i\omega r_*} + A_{\text{out}} e^{i\omega r_*}. \tag{F2}$$

Suppose for some particular ω_0 the ingoing wave is zero: $A_{\text{in}}(\omega_0) = 0$. So what is $dA_{\text{in}}/d\omega(\omega_0)$ in this case? To answer this question, we first define $\psi_1 = \psi$, $\psi_2 = \partial\psi/\partial r_*$ and $\vec{\psi} = (\psi_1, \psi_2)$, then we have

$$\begin{cases} \frac{\partial\psi_1}{\partial r_*} - \psi_2 = 0 \\ \frac{\partial\psi_2}{\partial r_*} + (\omega^2 - V)\psi_1 = 0, \end{cases} \tag{F3}$$

These equations can also be written as

$$\begin{pmatrix} \frac{\partial}{\partial r_*} & -1 \\ \omega^2 - V & \frac{\partial}{\partial r_*} \end{pmatrix} \begin{pmatrix} \psi_1 \\ \psi_2 \end{pmatrix} = \mathcal{O}\vec{\psi} = 0, \tag{F4}$$

and the boundary condition at infinity $r_* \rightarrow \infty$ is

$$\psi_1 \rightarrow A_{\text{in}} e^{-i\omega r_*} + A_{\text{out}} e^{i\omega r_*}, \tag{F5}$$

$$\psi_2 \rightarrow -i\omega A_{\text{in}} e^{-i\omega r_*} + i\omega A_{\text{out}} e^{i\omega r_*}. \tag{F6}$$

In order to compute $dA_{\text{in}}/d\omega(\omega_0)$, we define $\phi_1 = e^{-i\omega r_*}\psi_1$, and $\phi_2 = \partial\phi_1/\partial r_*$, then we can rewrite Eq. (F4) as

$$\begin{pmatrix} \frac{\partial}{\partial r_*} & -1 \\ -V & \frac{\partial}{\partial r_*} + 2i\omega \end{pmatrix} \begin{pmatrix} \phi_1 \\ \phi_2 \end{pmatrix} = \hat{\mathcal{O}}\vec{\phi} = 0. \tag{F7}$$

At infinity $r \rightarrow \infty$, $\vec{\phi}$ behave as

$$\phi_1 \rightarrow A_{\text{in}} e^{-2i\omega r_*} + A_{\text{out}}, \tag{F8}$$

$$\phi_2 \rightarrow -2i\omega A_{\text{in}} e^{-2i\omega r_*}. \tag{F9}$$

Now since $\hat{\mathcal{O}}(\omega_0)\vec{\phi}(\omega_0) = 0$, at $\omega = \omega_0 + \delta\omega$ we have $\vec{\phi}(\omega) = \vec{\phi}(\omega_0) + \delta\vec{\phi}$ and

$$\hat{\mathcal{O}}(\omega_0)\delta\vec{\phi} + \delta\omega \frac{\partial\hat{\mathcal{O}}}{\partial\omega}(\omega_0)\vec{\phi}(\omega_0) = 0, \tag{F10}$$

where

$$\frac{\partial\hat{\mathcal{O}}}{\partial\omega}(\omega_0) = \begin{pmatrix} 0 & 0 \\ 0 & 2i \end{pmatrix}. \tag{F11}$$

Here $\delta\phi$ can be solved by imposing the ingoing boundary condition

$$\begin{aligned} \frac{\delta\phi_1}{\delta\omega} &\rightarrow \frac{\delta A_{\text{in}}}{\delta\omega} e^{-2i\omega r_*} \left(\bar{a}_0 + \frac{\bar{a}_1}{r} + \frac{\bar{a}_2}{r^2} \right) + A_{\text{in}}(-2ir_*) e^{-2i\omega r_*} \left(\bar{a}_0 + \frac{\bar{a}_1}{r} + \frac{\bar{a}_2}{r^2} \right) \\ &\quad + A_{\text{in}} e^{-2i\omega r_*} \left(\bar{a}_0 + \frac{\bar{a}_1}{r} + \frac{\bar{a}_2}{r^2} \right)_{,\omega} + \frac{\delta A_{\text{out}}}{\delta\omega} \left(a_0 + \frac{a_1}{r} + \frac{a_2}{r^2} \right) + A_{\text{out}} \left(a_0 + \frac{a_1}{r} + \frac{a_2}{r^2} \right)_{,\omega}, \end{aligned} \quad (\text{F12})$$

$$\begin{aligned} \frac{\delta\phi_2}{\delta\omega} &\rightarrow \frac{\delta A_{\text{in}}}{\delta\omega} (-2i\omega) e^{-2i\omega r_*} \left(\bar{a}_0 + \frac{\bar{a}_1}{r} + \frac{\bar{a}_2}{r^2} \right) + A_{\text{in}}(-2i) e^{-2i\omega r_*} \left(\bar{a}_0 + \frac{\bar{a}_1}{r} + \frac{\bar{a}_2}{r^2} \right) \\ &\quad + A_{\text{in}}(-2i\omega)(-2ir_*) e^{-2i\omega r_*} \left(\bar{a}_0 + \frac{\bar{a}_1}{r} + \frac{\bar{a}_2}{r^2} \right) + A_{\text{in}}(-2i\omega) e^{-2i\omega r_*} \left(\bar{a}_0 + \frac{\bar{a}_1}{r} + \frac{\bar{a}_2}{r^2} \right)_{,\omega} \\ &\quad + \frac{\delta A_{\text{in}}}{\delta\omega} e^{-2i\omega r_*} \left(-\frac{\bar{a}_1}{r^2} - 2\frac{\bar{a}_2}{r^3} \right) \frac{dr}{dr_*} + A_{\text{in}}(-2ir_*) e^{-2i\omega r_*} \left(-\frac{\bar{a}_1}{r^2} - 2\frac{\bar{a}_2}{r^3} \right) \frac{dr}{dr_*} \\ &\quad + A_{\text{in}} e^{-2i\omega r_*} \left(-\frac{\bar{a}_1}{r^2} - 2\frac{\bar{a}_2}{r^3} \right)_{,\omega} \frac{dr}{dr_*} + \frac{\delta A_{\text{out}}}{\delta\omega} \left(-\frac{a_1}{r^2} - 2\frac{a_2}{r^3} \right) \frac{dr}{dr_*} + A_{\text{out}} \left(-\frac{a_1}{r^2} - 2\frac{a_2}{r^3} \right)_{,\omega} \frac{dr}{dr_*}, \end{aligned} \quad (\text{F13})$$

at $r \rightarrow \infty$. If $G(x, x')$ is the corresponding Green's function, then

$$\delta\phi = \delta\omega \int_{-\infty}^{\infty} dx' G(x, x') \frac{\partial \hat{\mathcal{O}}}{\partial \omega} \phi_0(x'), \quad (\text{F14})$$

and

$$\frac{dA_{\text{in}}}{d\omega}(\omega_0) = e^{2i\omega x} \int_{-\infty}^{\infty} dx' G(x, x') \frac{\partial \hat{\mathcal{O}}}{\partial \omega} \phi_0(x'), \quad x \rightarrow \infty. \quad (\text{F15})$$

For the relativistic star case, we may accordingly redefine the Zerilli master variable to be $Ze^{-i\omega r_*}$ and use the modified wave equation outside the star. Accordingly we expect

$$\frac{dA_{\text{in}}}{d\omega}(\omega_0) = e^{2i\omega r_*} \int_0^{\infty} dx' G(r_*, x') \frac{\partial \mathcal{L}}{\partial \omega} \phi_0(x'), \quad r_* \rightarrow \infty. \quad \text{where} \quad (\text{F16})$$

We can rewrite interior equations (A16), (A17), (A18) and (A19) as follows:

$$\frac{d\vec{u}}{dr} - \vec{M}(r, \omega)\vec{u}(r) := \mathcal{P}\vec{u} = 0. \quad (\text{F17})$$

Then similar to the above discussion, at $\omega = \omega_0 + \delta\omega$ we have $\vec{u} = \vec{u}_0 + \delta\vec{u}$ with $\vec{u}_0 = \{H_1^0, K^0, W^0, X^0\}$ a solution of the interior equations, and then we have

$$\mathcal{P}(\omega_0)\delta\vec{u} + \delta\omega \frac{\partial \mathcal{P}}{\partial \omega} \vec{u}_0 = 0, \quad (\text{F18})$$

$$\frac{\partial \mathcal{P}}{\partial \omega} = \left\{ \frac{e^\lambda}{r} \left[\frac{\delta H_0}{\delta\omega} - 16\pi(\varepsilon + p) \frac{\delta V}{\delta\omega} \right], \frac{1}{r} \frac{\delta H_0}{\delta\omega}, r e^{\lambda/2} \left[-\frac{\ell(\ell+1)}{r^2} \frac{\delta V}{\delta\omega} + \frac{1}{2} \frac{\delta H_0}{\delta\omega} \right], Q \right\}, \quad (\text{F19})$$

with

$$Q = (p + \varepsilon) e^{\nu/2} \left[\left(\frac{\nu'}{2} - \frac{1}{2r} \right) \frac{\delta H_0}{\delta\omega} - \frac{\ell(\ell+1)}{2r^2} \nu' \frac{\delta V}{\delta\omega} - \frac{2\omega}{r} e^{\lambda/2 - \nu} W^0 \right],$$

in which $\frac{\delta H_0}{\delta\omega}$ and $\frac{\delta V}{\delta\omega}$ are given by

$$\frac{\delta H_0}{\delta\omega} = \frac{1}{hr} \left(\frac{2\omega}{e^{\lambda+\nu}} H_1^0 - \frac{2\omega}{e^\lambda} K^0 \right), \quad (\text{F20})$$

$$\frac{\delta V}{\delta\omega} = -2\omega^{-3} \frac{e^{\nu/2} X^0}{\varepsilon + p} - 2\omega^{-3} \frac{e^{\nu/2}}{\varepsilon + p} \frac{1}{r} e^{\lambda+\nu} W^0, \quad (\text{F21})$$

$$- \frac{1}{2} e^\nu (-2\omega^{-3}) H_1^0 - \frac{1}{2} e^\nu \omega^{-2} \frac{\delta H_0}{\delta\omega},$$

$$hr = 3M(r) + \frac{1}{2}(\ell+2)(\ell-1)r + 4\pi r^3 p(r). \quad (\text{F22})$$

The boundary conditions of the above equations near the center $r = 0$,

$$\delta\vec{u}|_{\text{near center}} = \frac{d\vec{u}}{d\omega} \cdot \delta\omega|_{\text{near center}}. \quad (\text{F23})$$

As a result, we assume that the solutions are represented by power series expansions near the center $r = 0$, which are given by

$$\begin{aligned}\frac{\delta H_1}{\delta\omega} &= \frac{\delta y_0}{\delta\omega} + \frac{1}{2} \frac{\delta y_2}{\delta\omega} r^2 + \dots, \\ \frac{\delta K}{\delta\omega} &= \frac{\delta k_0}{\delta\omega} + \frac{1}{2} \frac{\delta k_2}{\delta\omega} r^2 + \dots, \\ \frac{\delta W}{\delta\omega} &= \frac{\delta w_0}{\delta\omega} + \frac{1}{2} \frac{\delta w_2}{\delta\omega} r^2 + \dots, \\ \frac{\delta X}{\delta\omega} &= \frac{\delta x_0}{\delta\omega} + \frac{1}{2} \frac{\delta x_2}{\delta\omega} r^2 + \dots.\end{aligned}\quad (\text{F24})$$

If we substitute Eqs. (F24) into Eqs. (F17) and solve the equations order by order, we can obtain the first order constraints $\mathcal{O}(r^0)$ and the second order constraints $\mathcal{O}(r^2)$. In particular, the first order constraints $\mathcal{O}(r^0)$, following these relations can be written as

$$\begin{aligned}\frac{\delta x_0}{\delta\omega} &= (\varepsilon_0 + p_0)e^{\nu_0/2} \left\{ \left[\frac{4\pi}{3}(\varepsilon_0 + 3p_0) - \omega^2 e^{-\nu_0}/\ell \right] \frac{\delta w_0}{\delta\omega} \right. \\ &\quad \left. + \frac{1}{2} \frac{\delta k_0}{\delta\omega} \right\} + (\varepsilon_0 + p_0)e^{\nu_0/2} (-2\omega e^{-\nu_0}/\ell) W_{r_0},\end{aligned}\quad (\text{F25})$$

$$\frac{\delta y_0}{\delta\omega} = \frac{2\ell \frac{\delta k_0}{\delta\omega} + 16\pi(\varepsilon_0 + p_0) \frac{\delta w_0}{\delta\omega}}{\ell(\ell + 1)}.\quad (\text{F26})$$

Let $\vec{u}_2 = \{y_2, k_2, w_2, x_2, \}$, then we can rewrite the Eqs. (36)-(39) in [34] as

$$\vec{F}(\omega)\vec{u}_2 = 0.\quad (\text{F27})$$

By implicit function theorem, $\frac{\delta y_2}{\delta\omega}$, $\frac{\delta k_2}{\delta\omega}$, $\frac{\delta w_2}{\delta\omega}$ and $\frac{\delta x_2}{\delta\omega}$ can be obtained.

For the even parity, the Zerilli function Z is related to interior perturbation functions at surface as

$$\begin{aligned}Z(r_*) &= -\frac{r^2 e^{-\lambda}}{nr + 3M} H_1 + \frac{r^2}{nr + 3M} K, \\ \frac{dZ(r_*)}{dr_*} &= \frac{n(n+1)r^2 + 3nMr + 6M^2}{(nr + 3M)^2} e^{-\lambda} H_1 \\ &\quad - \frac{nr^2 - 3nMr - 3M^2}{(nr + 3M)^2} K,\end{aligned}\quad (\text{F28})$$

which is evaluated at $r = R$. This can be rewritten as the form

$$\begin{pmatrix} Z \\ \frac{dZ(r_*)}{dr_*} \end{pmatrix} = \begin{pmatrix} A_{11} & A_{12} \\ A_{21} & A_{22} \end{pmatrix} \begin{pmatrix} H_1 \\ K \end{pmatrix}.\quad (\text{F30})$$

Then the relationship between $\delta\vec{\psi}$ and δH_1 , δK are

$$\begin{aligned}\delta\psi_1 &= A_{11}\delta H_1 + A_{12}\delta K + \frac{\partial A_{11}}{\partial\omega} H_1(\omega_0)\delta\omega \\ &\quad + \frac{\partial A_{12}}{\partial\omega} K(\omega_0)\delta\omega,\end{aligned}\quad (\text{F31})$$

$$\begin{aligned}\delta\psi_2 &= A_{21}\delta H_1 + A_{22}\delta K + \frac{\partial A_{21}}{\partial\omega} H_1(\omega_0)\delta\omega \\ &\quad + \frac{\partial A_{22}}{\partial\omega} K(\omega_0)\delta\omega.\end{aligned}\quad (\text{F32})$$

2. Shooting Method

Eqs. (F10 & F18) are nonhomogeneous differential equations. The boundary conditions include two regularity conditions at the center of the star, one condition $\delta X/\delta\omega = 0$ imposed at the stellar surface, and another condition $\delta A_{\text{out}}/\delta\omega = 0$ applied at spatial infinity. The shooting method, which transforms a boundary value problem into an initial value problem, can be employed to solve this system effectively.

We begin by making an initial guess for $\delta\vec{u}/\delta\omega(r_0)$ at the center and $\delta\vec{u}/\delta\omega(R)$ at the surface of the star. These two solutions must match at $r = R/2$. From there, we adjust our guess iteratively, refining the solution until the boundary conditions at both the center and the surface of the star are satisfied. Additionally, we ensure that $\delta A_{\text{out}}/\delta\omega = 0$ is correctly determined at infinity.

3. Results

In Table I, we list a set of numerical results for W_n (of f -modes) computed using the eigenfunction method, and compare them with the results obtained via the contour integral method described in Appendix B. In our calculations, we adopt a polytropic equation of state with $n = 1$ and fix the stellar mass $M = 1.4 M_\odot$, while vary the stellar radius R . It can be seen that the results obtained from the eigenfunction method agree remarkably well with those from the contour integral method, with typical relative differences on the order of 10^{-3} . The minor discrepancies observed are mainly attributed to variations in the numerical computation of the f -mode frequency.

REFERENCES

- [1] E. E. Flanagan and T. Hinderer, *Phys. Rev. D* **77**, 021502 (2008), arXiv:0709.1915 [astro-ph].
- [2] J. Steinhoff, T. Hinderer, A. Buonanno, and A. Taracchini, *Phys. Rev. D* **94**, 104028 (2016), arXiv:1608.01907 [gr-qc].
- [3] D. Lai, *Mon. Not. Roy. Astron. Soc.* **270**, 611 (1994), arXiv:astro-ph/9404062.
- [4] D. Lai and Y. Wu, *Phys. Rev. D* **74**, 024007 (2006), arXiv:astro-ph/0604163.
- [5] H. Yu and N. N. Weinberg, *Mon. Not. Roy. Astron. Soc.* **470**, 350 (2017), arXiv:1705.04700 [astro-ph.HE].
- [6] H. Yang, W. E. East, V. Paschalidis, F. Pretorius, and R. F. P. Mendes, *Phys. Rev. D* **98**, 044007 (2018), arXiv:1806.00158 [gr-qc].
- [7] H. Yang, *Phys. Rev. D* **100**, 064023 (2019), arXiv:1904.11089 [gr-qc].
- [8] Z. Pan, Z. Lyu, B. Bonga, N. Ortiz, and H. Yang, *Phys. Rev. Lett.* **125**, 201102 (2020), arXiv:2003.03330 [astro-ph.HE].
- [9] E. Poisson, *Phys. Rev. D* **101**, 104028 (2020), arXiv:2003.10427 [gr-qc].

M/R	$\text{Re}(W_n)$			$\text{Im}(W_n)$		
	Cont. Int.	Eigenfunc.	Rel. Diff.	Cont. Int.	Eigenfunc.	Rel. Diff.
0.1736	3.00578×10^{-5}	3.01606×10^{-5}	0.00342	4.32034×10^{-5}	4.31338×10^{-5}	0.00161
0.1491	1.82786×10^{-5}	1.83621×10^{-5}	0.00456	2.92974×10^{-5}	2.92457×10^{-5}	0.00177
0.1202	8.13349×10^{-6}	8.19500×10^{-6}	0.00756	1.57176×10^{-5}	1.56856×10^{-5}	0.00204
0.1016	4.08830×10^{-6}	4.07389×10^{-6}	0.00352	9.28618×10^{-6}	9.31389×10^{-6}	0.00298
0.0799	1.43370×10^{-6}	1.43332×10^{-6}	0.00027	4.16154×10^{-6}	4.16166×10^{-6}	0.00003
0.0502	1.65314×10^{-7}	1.65194×10^{-7}	0.00073	7.93831×10^{-7}	7.93855×10^{-7}	0.00003
0.0304	1.41535×10^{-8}	1.40133×10^{-8}	0.01000	1.20746×10^{-8}	1.20776×10^{-8}	0.00025
0.0185	1.15318×10^{-9}	1.12708×10^{-9}	0.02315	1.77977×10^{-8}	1.78004×10^{-8}	0.00015
0.0103	5.62403×10^{-11}	5.69662×10^{-11}	0.01274	1.79181×10^{-9}	1.79306×10^{-9}	0.00070
0.0062	3.88375×10^{-12}	3.22998×10^{-12}	0.20241	2.37554×10^{-10}	2.37565×10^{-10}	0.00005

Table I. The values of W_n (for f-modes) as a function of the compactness of the neutron star, computed using two independent numerical methods: the contour integral method (Appendix B) and the eigenfunction method (Appendix F). The stellar models are constructed using a polytropic equation of state with index $n = 1$, with the mass fixed at $M = 1.4 M_\odot$ and the radius R varied over a range of values. The results from the two methods show excellent agreement, with relative differences typically at the level of 10^{-3} .

- [10] S. Ma, H. Yu, and Y. Chen, *Phys. Rev. D* **103**, 063020 (2021), arXiv:2010.03066 [gr-qc].
- [11] S. Y. Lau and K. Yagi, *Phys. Rev. D* **103**, 063015 (2021), arXiv:2012.13000 [astro-ph.HE].
- [12] K. J. Kwon, H. Yu, and T. Venumadhav, (2024), arXiv:2410.03831 [gr-qc].
- [13] K. J. Kwon, H. Yu, and T. Venumadhav, (2025), arXiv:2503.11837 [gr-qc].
- [14] Z. Miao, E. Zhou, and A. Li, *Astrophys. J.* **964**, 31 (2024), arXiv:2305.08401 [nucl-th].
- [15] M. Shibata and K. Taniguchi, *Phys. Rev. D* **73**, 064027 (2006), arXiv:astro-ph/0603145.
- [16] K. Kiuchi, Y. Sekiguchi, M. Shibata, and K. Taniguchi, *Phys. Rev. D* **80**, 064037 (2009), arXiv:0904.4551 [gr-qc].
- [17] A. Bauswein and H. T. Janka, *Phys. Rev. Lett.* **108**, 011101 (2012), arXiv:1106.1616 [astro-ph.SR].
- [18] A. Bauswein, N. Stergioulas, and H.-T. Janka, *Eur. Phys. J. A* **52**, 56 (2016), arXiv:1508.05493 [astro-ph.HE].
- [19] C. Palenzuela, S. L. Liebling, D. Neilsen, L. Lehner, O. L. Caballero, E. O'Connor, and M. Anderson, *Phys. Rev. D* **92**, 044045 (2015), arXiv:1505.01607 [gr-qc].
- [20] H. Yang, V. Paschalidis, K. Yagi, L. Lehner, F. Pretorius, and N. Yunes, *Phys. Rev. D* **97**, 024049 (2018), arXiv:1707.00207 [gr-qc].
- [21] L. Baiotti and L. Rezzolla, *Rept. Prog. Phys.* **80**, 096901 (2017), arXiv:1607.03540 [gr-qc].
- [22] V. Paschalidis and N. Stergioulas, *Living Rev. Rel.* **20**, 7 (2017), arXiv:1612.03050 [astro-ph.HE].
- [23] H. Miao, H. Yang, and D. Martynov, *Phys. Rev. D* **98**, 044044 (2018), arXiv:1712.07345 [gr-qc].
- [24] D. Martynov *et al.*, *Phys. Rev. D* **99**, 102004 (2019), arXiv:1901.03885 [astro-ph.IM].
- [25] T. Zhang, H. Yang, D. Martynov, P. Schmidt, and H. Miao, *Phys. Rev. X* **13**, 021019 (2023), arXiv:2212.12144 [gr-qc].
- [26] T. Hinderer, *Astrophys. J.* **677**, 1216 (2008), [Erratum: *Astrophys. J.* 697, 964 (2009)], arXiv:0711.2420 [astro-ph].
- [27] T. Hinderer *et al.*, *Phys. Rev. Lett.* **116**, 181101 (2016), arXiv:1602.00599 [gr-qc].
- [28] B. P. Abbott *et al.* (LIGO Scientific, Virgo), *Phys. Rev. Lett.* **119**, 161101 (2017), arXiv:1710.05832 [gr-qc].
- [29] K. D. Kokkotas and B. G. Schmidt, *Living Rev. Rel.* **2**, 2 (1999), arXiv:gr-qc/9909058.
- [30] T. Pitre and E. Poisson, *Phys. Rev. D* **109**, 064004 (2024), arXiv:2311.04075 [gr-qc].
- [31] E. W. Leaver, *Phys. Rev. D* **34**, 384 (1986).
- [32] V. Moncrief, *Annals Phys.* **88**, 323 (1974).
- [33] V. Moncrief, *Annals Phys.* **88**, 343 (1974).
- [34] X. Feng and H. Yang, *Phys. Rev. D* **110**, 044066 (2024), arXiv:2406.02101 [gr-qc].
- [35] T. Regge and J. A. Wheeler, *Phys. Rev.* **108**, 1063 (1957).
- [36] F. J. Zerilli, *Phys. Rev. Lett.* **24**, 737 (1970).
- [37] F. J. Zerilli, *Phys. Rev. D* **2**, 2141 (1970).
- [38] H. Onozawa, *Phys. Rev. D* **55**, 3593 (1997), arXiv:gr-qc/9610048.
- [39] G. B. Cook and M. Zalutskiy, *Phys. Rev. D* **90**, 124021 (2014), arXiv:1410.7698 [gr-qc].
- [40] E. Berti, V. Cardoso, K. D. Kokkotas, and H. Onozawa, *Phys. Rev. D* **68**, 124018 (2003), arXiv:hep-th/0307013.
- [41] H. Motohashi, *Phys. Rev. Lett.* **134**, 141401 (2025), arXiv:2407.15191 [gr-qc].
- [42] K. S. Thorne, *Rev. Mod. Phys.* **52**, 299 (1980).
- [43] S. Ma and H. Yang, *Phys. Rev. D* **109**, 104070 (2024), arXiv:2401.15516 [gr-qc].
- [44] H. Yang, A. Zimmerman, and L. Lehner, *Phys. Rev. Lett.* **114**, 081101 (2015), arXiv:1402.4859 [gr-qc].
- [45] M. M. Ivanov and Z. Zhou, *Phys. Rev. Lett.* **130**, 091403 (2023), arXiv:2209.14324 [hep-th].
- [46] A. Le Tiec, L. Blanchet, and B. F. Whiting, *Phys. Rev. D* **85**, 064039 (2012), arXiv:1111.5378 [gr-qc].
- [47] A. Le Tiec, E. Barausse, and A. Buonanno, *Phys. Rev. Lett.* **108**, 131103 (2012), arXiv:1111.5609 [gr-qc].
- [48] S. L. Detweiler, *Phys. Rev. D* **77**, 124026 (2008), arXiv:0804.3529 [gr-qc].
- [49] E. Barausse, A. Buonanno, and A. Le Tiec, *Phys. Rev. D* **85**, 064010 (2012), arXiv:1111.5610 [gr-qc].
- [50] A. Buonanno and T. Damour, *Phys. Rev. D* **59**, 084006 (1999), arXiv:gr-qc/9811091.
- [51] T. Damour, P. Jaranowski, and G. Schaefer, *Phys. Rev. D* **62**, 084011 (2000), arXiv:gr-qc/0005034.
- [52] D. Bini, T. Damour, and G. Faye, *Phys. Rev. D* **85**, 124034 (2012), arXiv:1202.3565 [gr-qc].

- [53] X. Feng, Z. Lyu, and H. Yang, *Phys. Rev. D* **105**, 104043 (2022), [arXiv:2104.11848 \[gr-qc\]](#).
- [54] A. Pound, B. Wardell, N. Warburton, and J. Miller, *Phys. Rev. Lett.* **124**, 021101 (2020), [arXiv:1908.07419 \[gr-qc\]](#).
- [55] L. Lindblom and S. L. Detweiler, *Astrophys. J. Suppl.* **53**, 73 (1983).